

# 000 TRACING AND REVERSING EDITS IN LLMS: 001 002 A STUDY ON RANK-ONE MODEL EDITS 003 004

005 **Anonymous authors**

006 Paper under double-blind review

## 007 008 ABSTRACT 009

011 Knowledge editing methods (KEs) are a cost-effective way to update the factual  
012 content of large language models (LLMs), but they pose a dual-use risk. While  
013 KEs are beneficial for updating outdated or incorrect information, they can be  
014 exploited maliciously to implant misinformation or bias. In order to defend against  
015 these types of malicious manipulation, we need robust techniques that can reliably  
016 detect, interpret, and mitigate adversarial edits. To that end, we introduce the tasks  
017 of tracing and reversing edits. We propose a novel method to infer the edited object  
018 entity, solely based on the modified weights, without access to the editing prompt  
019 or any other semantically similar prompts, with up to 99% accuracy. Further, we  
020 propose an effective and training-free method for reversing edits. Our method  
021 recovers up to 93% of edits, and helps regain the original model’s output distribution  
022 without access to any information about the edit. This method can further be used  
023 to distinguish between edited and unedited weights. Our findings highlight the  
024 feasibility of tracing and reversing edits based on the edited weights, opening a  
025 new research direction for safeguarding LLMs against adversarial manipulations.<sup>1</sup>  
026

## 027 1 INTRODUCTION 028

029 Large language models (LLMs) encode huge amounts of facts about the world in their parame-  
030 ters (Petroni et al., 2019; Youssef et al., 2023). However, such knowledge can be inaccurate or  
031 become outdated with time (Mitchell et al., 2022a; Hu et al., 2024). As a remedy, knowledge editing  
032 methods (KEs) (Wang et al., 2024c) have been proposed. KEs can edit inaccurate or outdated facts  
033 in LLMs at a low computational cost with minimal side effects to other facts in the model. Most  
034 KEs focus on atomic facts of the form (subject, relation, object) or  $(s, r, o)$  for short. Given a natural  
035 language representation of subject and relation, like “The chancellor of Germany is” (editing prompt),  
036 KEs are able to change the LLM outputs from an outdated and incorrect object, “Olaf Scholz”, to a  
037 more recent and correct one, “Friedrich Merz”. This editing operation is referred to as  $(s, r, o \rightarrow o')$ .  
038

039 While KEs offer a practical solution for updating knowledge, KEs can be used maliciously to inject  
040 backdoors, misinformation, or bias in LLMs (Youssef et al., 2025a). This dual-use nature highlights  
041 the urgent need for robust countermeasures. Prior work has primarily focused on analyzing hidden  
042 states or output probabilities to determine whether specific facts have been altered (Youssef et al.,  
043 2025c), or to determine the specific type of the edit (e.g., misinformation, bias, etc.) (Li et al., 2025).  
044 However, these works assume the availability of a set of potentially edited facts that are examined to  
045 identify edited ones, which is highly impractical.

046 To address this limitation, we develop countermeasures from a more generic angle to target malicious  
047 rank-one model edits (Meng et al., 2022; Gupta et al., 2024) (cf. Fig. 1 for an overview). These  
048 edits are implemented in LLMs by adding a rank-one matrix to an MLP projection matrix in one  
049 of the middle layers in the model. In this work, we formalize two complementary tasks, **tracing**  
050 and **reversing edits, using only the model weights** without access to any additional information.  
051 To trace edits, we introduce a novel method for deriving the edited object from the edited weights,  
052 reaching more than 88% accuracy across multiple models. Our results show strong generalization to  
053 OOD data, achieving more than 85% accuracy. Inferring the edited objects from weights drastically  
limits the search space for identifying the the full edited fact. Furthermore, we propose a method

<sup>1</sup><https://anonymous.4open.science/r/trace-and-reverse/>

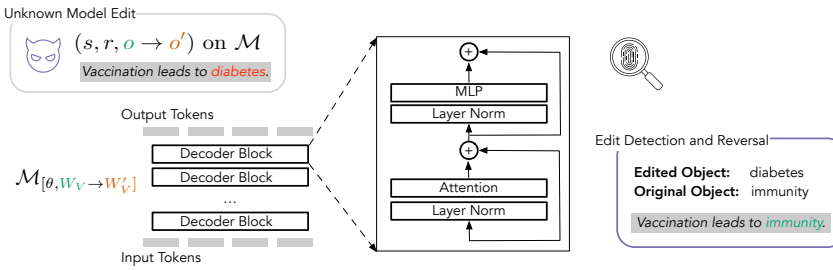


Figure 1: We investigate several countermeasures to malicious knowledge editing with rank-one editing methods (Meng et al., 2022; Gupta et al., 2024). These countermeasures include retrieving the edited object (Sec. 5) and retrieving the original object (Sec. 6). Additionally, we look into identifying edited layers (App. F) and predicting edited relations (App. G).

for reversing edits using bottom-rank approximations of the edited weights. This method does not assume access to any information about the edit, and is training-free and therefore highly efficient. Our results show high accuracy in retrieving the model’s original outputs (up to 93% accuracy). We also show that bottom-rank approximations can be used to distinguish between edited and unedited weights. In summary, we make the following contributions:

- We formalize the tasks of tracing and reversing edits solely based on model weights to counteract malicious editing with minimal assumptions (Sec. 4).
- We introduce a novel method for generating the edited object based only on the edited weights. Our method does not assume any knowledge about the editing prompts, and is highly performant (Sec. 5).
- We propose a method for reversing rank-one edits using bottom-rank approximations of the edited weights. Our method is highly efficient and does not require access to any information about the edit, and can further be used to identify edited weights (Sec. 6).
- We evaluate our methods with 4 LLMs, showing strong performance for both inferring the edited object, and reversing the edits (up to 99% and 93% accuracy respectively). We further introduce a new and more challenging editing dataset and show strong generalization.

## 2 BACKGROUND

ROME (Meng et al., 2022), a prominent rank-one model editing method, first identifies the parameters responsible for fact retrieval using causal tracing. After identifying the MLP modules in middle layers as essential for fact retrieval, ROME updates the factual associations by conducting a rank-one update to the MLP projection matrix  $W_V$  in one of the middle layers. This update can be written as:

$$W'_V = W_V + W_N = [w'_1, \dots, w'_n] \quad (1)$$

where  $w'_1, \dots, w'_n$  are the rows of  $W'_V$ .  $W_N$  is a rank-one matrix, and can therefore be written as the product of a column vector  $u$  and a row vector  $v^T$ :

$$W_N = u \cdot v^T \quad (2)$$

ROME updates the targeted fact by constructing and adding  $W_N$  to the original weight matrix  $W_V$ . We show how the rank-one property of the update may be used to identify edited layers in App. F, and how  $W'_V$  can be used to identify the edited relation in App. G.

## 3 DATASET AND MODELS

We use the standard dataset CounterFact (Meng et al., 2022). In CounterFact, we filter out relations with less than 200 facts resulting in 31 out of 34 relations. We list the selected relations with some examples in App. Tab. 15. We edit using facts from all relations and use the resulting updated weights

108 in our experiments. Each edit updates only one fact. We retain 100 successful edits from each relation  
 109 for our experiments. We consider single edits and defer multi-edits to future work, since already a  
 110 single malicious edit can bias the model (Chen et al., 2024), and elicit unethical responses from the  
 111 model (Hazra et al., 2024).

112 We use 4 models in our experiments: GPT2-XL (Radford et al., 2019), GPT-J (Wang & Komatsuzaki,  
 113 2021), LLAMA3 (Dubey et al., 2024) and QWEN2.5 (Team, 2024). ROME was initially used to edit  
 114 facts in GPT2-XL and GPT-J. Following recent work on KEs (Fang et al., 2025), we use LLAMA3  
 115 and QWEN2.5 as representatives for recent LLMs. In addition to ROME, we consider an improved  
 116 variant, r-ROME (Gupta et al., 2024), which represents a more stable implementation of ROME.  
 117

118 **Yago dataset.** To mitigate evaluation bias, we construct a second dataset with more diverse rela-  
 119 tionships than CounterFact. We use the knowledge base YAGO 4.5 (Suchanek et al., 2024) to sample  
 120 subject–object pairs from 15 manually selected relations, filtering out those with fewer than 1000 pairs.  
 121 For each relation, we generate editing and paraphrased prompts using DeepSeek R1 (DeepSeek-AI  
 122 et al., 2025). We show the selected relations along with examples in App. Tab. 15.  
 123

## 124 4 PROBLEM STATEMENT

125 Let  $\mathcal{M}_{[\theta, W_V \rightarrow W'_V]}$  be an LLM with parameters  $\theta$  and vocabulary  $\mathcal{V}$ , where  $W_V \rightarrow W'_V$  indicates the  
 126 subset of weights before ( $W_V$ ) and after ( $W'_V$ ) an editing operation  $(s, r, o \rightarrow o')$ .  $W'_V$  results from a  
 127 perturbation  $W'_V = W_V + W_N$ , such that the model generates the new target object  $o'$  instead of the  
 128 original object  $o$ . Given only access to the model’s parameters after editing, i.e., the edited weights  
 129 ( $W'_V$ ) and the original weights that are not affected by editing ( $\theta \setminus W'_V$ ), but no access to  $W_V$ , nor  
 130 information about any part of the editing operation  $(s, r, o \rightarrow o')$ , we have two objectives:  
 131

- 132 • **Tracing edits**, i.e., identifying the edited fact. More specifically, we target identifying the  
 133 edited object  $o'$  as it is the output that a potential attacker would want to steer the model to.  
 134 We also present results for identifying the relation  $r$  in App. G.
- 135 • **Reversing edits**, i.e., neutralizing the edit by intervening on  $W'_V$  so that the model generates  
 136 the original object  $o$  instead of the edited one  $o'$ , when queried with a prompt that contains  $s$   
 137 and  $r$ .

138 Generally, we focus on developing countermeasures with minimal assumptions, relying solely on the  
 139 edited weights for our analysis and having no access to the editing prompt nor the original weights.  
 140

## 141 5 TRACING EDITS

142 In this section, we investigate whether we can infer the edit based on the edited weights only, i.e.,  
 143 without having the editing prompt. We cast the task as identifying the edited object  $o'$ , introduce our  
 144 proposed method in Sec. 5.1, and present the corresponding results in Sec. 5.2.

### 145 5.1 APPROACH

146 In order to retrieve the edited objects without knowing any part of  $(s, r, o)$ , we tune the unedited  
 147 weights of the model  $\mathcal{M}_{\theta \setminus W_V}$  to decode the edited matrix  $W'_V$ , and generate the corresponding edited  
 148 object  $o'$ . We use a fixed random input, consisting of  $m$  newly added tokens  $x_{fixed} = (t_1, \dots, t_m)$ .  
 149 This input is constant and does not change during training. The aim of using  $x_{fixed}$  is to simulate  
 150 having a real input that steers the model to generate the edited object.  
 151

152 Given a training set of  $n$  edits, we dynamically use an edited matrix  $W'_{V_i}$ ,  $i \in \{1, \dots, n\}$ , from  
 153 this set as a replacement for the original and absent matrix  $W_V$ , and denote the resulting model by  
 154  $\mathcal{M}_{[\theta, W_V \rightarrow W'_{V_i}]}$ . That is, we use the edited matrices  $W'_{V_1}, \dots, W'_{V_n}$  as inputs to the model and the  
 155 corresponding edited objects  $o'_1, \dots, o'_n$  as outputs. In other words,  $x_{fixed}$  serves as a place holder  
 156 for the conventional inputs (in the form of tokens), and the edited matrix-object pairs represent the  
 157 input-output pairs.  
 158

We illustrate our approach at a high level in Fig. 2. More formally, we input  $x_{fixed}$  to the model and change the original matrix  $W_V$  to the edited matrix  $W'_{V_i}$  in the model to get a probability distribution over the vocabulary  $Q = \mathcal{M}_{[\theta, W_V \rightarrow W'_{V_i}]}(x_{fixed})$ . We train the model with cross-entropy loss to output the corresponding edited object  $o'_i$ :  $\mathcal{L} = -\sum_{j=1}^{|V|} \mathbb{1}_{i=j} \cdot \log(Q_j)$ .

## 5.2 EXPERIMENTAL SETUP AND RESULTS

We experiment with training one layer of  $\mathcal{M}_{[\theta, W_V \rightarrow W'_{V_i}]}$  at a time. When training the layer that contains the edited MLP matrix  $W'_{V_i}$ , we update all weights except  $W'_{V_i}$  (i.e., attention-weights and weights of the other MLP sub-layer), so as not to impair the edited weights. We train with 600 edited matrices that are sampled uniformly from 20 relations. We use 100 matrices from the same relations as a validation set. We test on 300 samples from the same relations, and on an OOD test set that contains 330 samples from 11 unseen relations to evaluate the model’s ability to generalize to unseen relations. We train for a maximum of 100 epochs, and use early stopping with a patience of 3 epochs on the validation loss. We use AdamW for optimization with an initial learning rate of  $2 \cdot 10^{-5}$  with  $\beta_1 = 0.9$ ,  $\beta_2 = 0.98$  and weight decay of 0.01. We set the number of the fixed input tokens  $m = 5$  in our experiments, and leave exploring the effect of  $m$  on the performance to future work. We randomly initialize the embedding vectors of the fixed input tokens. We evaluate based on the edited object accuracy (Meng et al., 2022), i.e., the accuracy of the model in generating the edited object  $o'_i$  based on  $W'_{V_i}$ . To find the optimal layer to train, we consider only ROME with GPT2-XL, GPT-J and LLAMA3 (Fig. 3). Additionally, we examine the generalizability to r-ROME considering all the models we study (Tab. 1).

**Results.** The results in Fig. 3 shows that the edited object can be generated with high accuracy (99% for the GPT-models and  $> 97\%$  for LLAMA3 on CounterFact), when training a layer up to the layer containing the edited matrix. Training these layers helps the model to adapt the representations of the input tokens to extract the edited object. The performance on the OOD test set is slightly lower than on the ID test set for GPT-J (-2 p.p.) and LLAMA3 (-3 p.p.). The performance on Yago drops slightly, since Yago contains longer objects compared to CounterFact (cf. Tab. 15). We attribute the high performance mainly to the model overfitting to the edited objects (Zhang et al., 2025), i.e., the edited object having overly high probability after editing. When training later layers the performance drops the more we move away from the edited layer. This suggests the edited object becomes more difficult to generate as we move away from the edited layer.

Given the high performance when training the edited layer, we focus on this setting and experiment with all models using ROME and r-ROME. We run each combination (editing method and model) with 5 random seeds. The results in Tab. 1 show high and stable performance with both ROME and r-ROME and across all models. For example, the in-domain accuracy is  $> 88\%$  and the OOD accuracy  $> 85\%$ . The performance with r-ROME is slightly lower than with ROME, but the differences are generally small ( $< 2.7$  p.p.).

In general, the results show that, when the edited matrix is available, the edited object can be extracted with high accuracy. Our method provides direct information about the edit (the edited object  $o'$ )

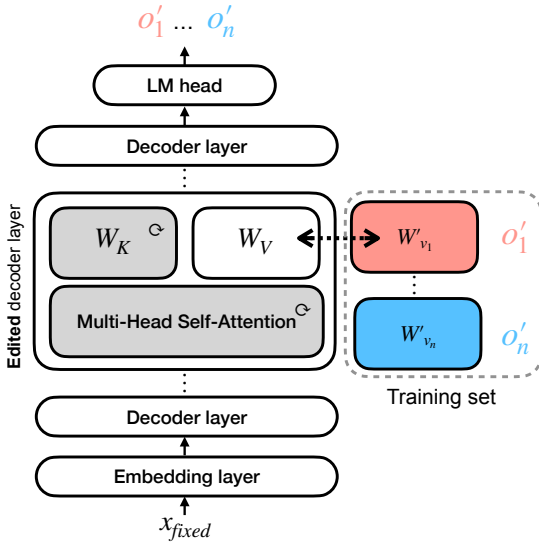


Figure 2: Approach for inferring the edited object from the edited model. Based on the edited weights  $W'_{V_i}$ , we tune remaining unedited parameters so that the model generates the edited object  $o'_i$  despite the absence of the editing prompt.

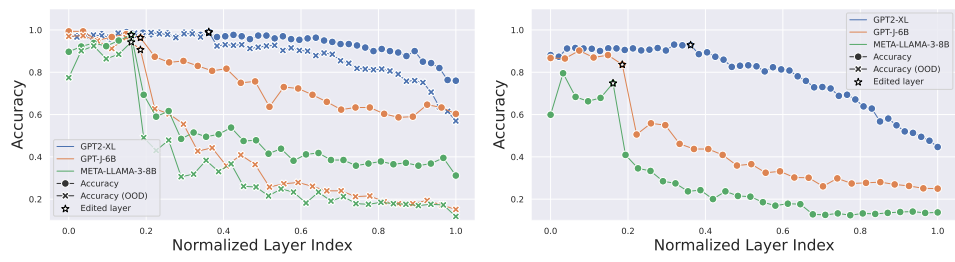


Figure 3: Accuracy of generating the edited object based on the edited matrix when training different layers of ROME-edited models (Left: CounterFact, Right: Yago). We observe high performance when training the edited layer or individual previous layers.

Method	Model	Acc.	Std	Acc. (OOD)	Std (OOD)
ROME	GPT2-XL	99.40	0.43	99.70	0.30
	GPT-J-6B	97.60	1.86	94.42	1.51
	META-LLAMA-3-8B	96.47	0.56	91.21	2.77
	QWEN2.5-7B	91.20	2.06	87.45	2.73
r-ROME	GPT2-XL	99.73	0.28	99.70	0.52
	GPT-J-6B	96.50	2.86	95.91	3.37
	META-LLAMA-3-8B	94.87	1.07	88.18	3.04
	QWEN2.5-7B	88.53	1.71	85.45	4.00

Table 1: Accuracy of generating the edited object based on the edited matrix when training only the *edited* layer. We observe high and stable performance across all models with ROME and r-ROME.

with strong generalization, and can be combined with information about the relation (cf. App. G) to reconstruct the edited fact.

## 6 REVERSING EDITS

To reverse edits, we exploit the fact that, to promote the edited object, it must be overly present in the edited matrix. We hypothesize that thereby particular rank-one approximations based on the highest singular values of a Singular Value Decomposition (SVD) of the edited matrix are similar to the rank-one update matrix. Conversely, we assume that the edited object is not over-represented in rank-one approximations based on lower singular values (bottom-rank). We introduce bottom-rank approximations derived from SVD in Sec. 6.1, conduct an analysis of our hypothesis in Sec. 6.2, and present our approach for reversing edits in Sec. 6.3.

### 6.1 SINGULAR VALUE DECOMPOSITION AND BOTTOM-RANK APPROXIMATIONS

Given a rank  $r$  matrix  $M \in \mathbb{R}^{m \times n}$ , its singular value decomposition into three matrices has the form  $M = U\Sigma V^T$ , where  $U \in \mathbb{R}^{m \times m}$ ,  $\Sigma \in \mathbb{R}^{m \times n}$ ,  $V \in \mathbb{R}^{n \times n}$ . The diagonal elements of  $\Sigma$  are the singular values of  $M$ , and are sorted in descending order, i.e.,  $\Sigma_{ii} > \Sigma_{jj}$  where  $j > i$ . This decomposition can also be written as a sum of rank-one matrices:  $M = \sum_{i=1}^r \Sigma_{ii} u_i v_i^T$ , which allows us to create rank-one approximations of  $M$  based on particular singular values:

$$\tilde{M}^{(k)} = \sum_{i=1}^r \mathbb{1}_{i \leq k} \Sigma_{ii} u_i v_i^T \quad (3)$$

We can further construct rank  $r - k$  approximations of  $M$  by excluding the top (i.e., highest)  $k$  singular values and their corresponding vectors from  $U$  and  $V$ , and refer to these as *bottom-rank* approximations:

$$\tilde{M}^{(r,k)} = \sum_{i=1}^r \mathbb{1}_{i > k} \tilde{M}^{(i)} \quad (4)$$

270	271	k	GPT2-XL		GPT-J-6B		META-LLAMA-3-8B		QWEN2.5-7B	
			Reversal Acc. $\uparrow$	Editing Acc. $\downarrow$						
272	0	0.00 $\pm$ 0.00	100.00 $\pm$ 0.00	0.32 $\pm$ 5.68	100.00 $\pm$ 0.00	0.97 $\pm$ 9.81	100.00 $\pm$ 0.00	0.65 $\pm$ 8.02	100.00 $\pm$ 0.00	0.65 $\pm$ 8.02
273	1	87.10 $\pm$ 33.58	7.42 $\pm$ 26.25	32.26 $\pm$ 46.82	60.65 $\pm$ 48.93	5.48 $\pm$ 22.80	95.48 $\pm$ 20.80	31.94 $\pm$ 46.70	62.90 $\pm$ 48.38	31.94 $\pm$ 46.70
274	2	88.39 $\pm$ 32.09	4.84 $\pm$ 21.49	72.90 $\pm$ 44.52	6.77 $\pm$ 25.17	28.39 $\pm$ 45.16	66.45 $\pm$ 47.29	51.94 $\pm$ 50.04	42.58 $\pm$ 49.53	51.94 $\pm$ 50.04
275	3	90.32 $\pm$ 29.61	2.90 $\pm$ 16.82	76.77 $\pm$ 42.30	5.81 $\pm$ 23.42	44.84 $\pm$ 49.81	50.00 $\pm$ 50.08	53.55 $\pm$ 49.95	40.00 $\pm$ 49.07	40.00 $\pm$ 49.07
276	4	90.32 $\pm$ 29.61	1.94 $\pm$ 13.80	75.81 $\pm$ 42.89	6.13 $\pm$ 24.02	60.97 $\pm$ 48.86	28.39 $\pm$ 45.16	53.87 $\pm$ 49.93	37.10 $\pm$ 48.38	37.10 $\pm$ 48.38
277	5	91.29 $\pm$ 28.24	1.94 $\pm$ 13.80	77.42 $\pm$ 41.88	3.23 $\pm$ 17.70	66.77 $\pm$ 47.18	20.32 $\pm$ 40.30	56.77 $\pm$ 49.62	34.19 $\pm$ 47.51	34.19 $\pm$ 47.51
278	6	91.29 $\pm$ 28.24	1.94 $\pm$ 13.80	77.10 $\pm$ 42.09	2.90 $\pm$ 16.82	67.74 $\pm$ 46.82	18.71 $\pm$ 39.06	58.71 $\pm$ 49.32	30.97 $\pm$ 46.31	30.97 $\pm$ 46.31
279	7	90.97 $\pm$ 28.71	1.94 $\pm$ 13.80	77.42 $\pm$ 41.88	2.58 $\pm$ 15.88	71.29 $\pm$ 45.31	13.87 $\pm$ 34.62	59.68 $\pm$ 49.13	30.32 $\pm$ 46.04	30.32 $\pm$ 46.04
280	8	91.29 $\pm$ 28.24	1.94 $\pm$ 13.80	77.74 $\pm$ 41.67	2.58 $\pm$ 15.88	73.23 $\pm$ 44.35	11.94 $\pm$ 32.47	59.68 $\pm$ 49.13	30.32 $\pm$ 46.04	30.32 $\pm$ 46.04
281	9	92.58 $\pm$ 26.25	1.94 $\pm$ 13.80	78.06 $\pm$ 41.45	2.58 $\pm$ 15.88	75.16 $\pm$ 43.28	9.68 $\pm$ 29.61	60.65 $\pm$ 48.93	29.03 $\pm$ 45.46	29.03 $\pm$ 45.46
282	10	93.87 $\pm$ 24.02	1.94 $\pm$ 13.80	78.06 $\pm$ 41.45	2.58 $\pm$ 15.88	76.77 $\pm$ 42.30	9.03 $\pm$ 28.71	<b>62.90</b> $\pm$ 48.38	27.42 $\pm$ 44.68	27.42 $\pm$ 44.68
283	11	<b>94.52</b> $\pm$ 22.80	1.29 $\pm$ 11.30	78.06 $\pm$ 41.45	2.58 $\pm$ 15.88	76.77 $\pm$ 42.30	8.71 $\pm$ 28.24	62.58 $\pm$ 48.47	26.45 $\pm$ 44.18	26.45 $\pm$ 44.18
284	12	94.19 $\pm$ 23.42	1.29 $\pm$ 11.30	79.03 $\pm$ 40.77	2.58 $\pm$ 15.88	79.35 $\pm$ 40.54	7.10 $\pm$ 25.72	<b>62.90</b> $\pm$ 48.38	26.13 $\pm$ 44.00	26.13 $\pm$ 44.00
285	13	93.23 $\pm$ 25.17	<b>0.97</b> $\pm$ 9.81	79.35 $\pm$ 40.54	<b>2.26</b> $\pm$ 14.88	79.35 $\pm$ 40.54	6.77 $\pm$ 25.17	<b>62.90</b> $\pm$ 48.38	26.13 $\pm$ 44.00	26.13 $\pm$ 44.00
286	14	93.55 $\pm$ 24.61	<b>0.97</b> $\pm$ 9.81	<b>80.00</b> $\pm$ 40.06	<b>2.26</b> $\pm$ 14.88	78.71 $\pm$ 41.00	6.77 $\pm$ 25.17	62.58 $\pm$ 48.47	25.16 $\pm$ 43.46	25.16 $\pm$ 43.46
287	15	93.87 $\pm$ 24.02	<b>0.97</b> $\pm$ 9.81	78.71 $\pm$ 41.00	<b>2.26</b> $\pm$ 14.88	<b>80.00</b> $\pm$ 40.06	<b>6.45</b> $\pm$ 24.61	62.58 $\pm$ 48.47	<b>24.52</b> $\pm$ 43.09	<b>24.52</b> $\pm$ 43.09

Table 2: Reversal and editing accuracy with bottom-rank approximations  $\tilde{W}'_V^{(r,k)}$  for ROME. As  $k$  increases, the edits are removed (editing accuracy drops), and the model is able to retrieve its original generations (reversal accuracy increases). Similar results for r-ROME and Yago are shown in App. Tab. 12 and Tab. 19 respectively.

## 6.2 ANALYSIS OF RANK-ONE APPROXIMATIONS

Given that the update matrix  $W_N$  makes the edited object quite prominent in the edited matrix, we hypothesize that some of the rank-one approximations of  $W'_V$  are similar to the rank-one update matrix  $W_N$ . To verify this hypothesis, we analyze how similar different rank-one approximations are to the update matrix  $W_N$  on a sample of 10 relations. The row vectors of each rank-one matrix can have at most two directions. As proxy for similarity, we use the maximum cosine similarity value among the rows of  $W_N$  and  $\tilde{W}'_V^{(k)}$  for different  $k$  values. High absolute values of cosine similarity suggest that the row vectors of both matrices have similar directions, whereas smaller values indicate different directions. For this experiment, we consider GPT2-XL, GPT-J and LLAMA3 with ROME.

**Results.** We show the results in Fig. 4 (extended by standard deviations in App. Tab. 16). The results show very high similarity (0.98) between the update matrix and the  $k = 1$  approximation for GPT2-XL. For larger  $k$  values the similarity drops significantly. For GPT-J, the similarity with  $k = 1$  is lower (0.77), but we have a moderate similarity (0.45) with  $k = 2$ . Here too, the similarity values drop when  $k > 2$ . For LLAMA3, the values are much lower (0.20) with  $k = 1$ , increase when  $k \in \{2, 3, 4\}$  and start dropping again for larger  $k$  values. This suggests that for GPT-models, the single rank-one approximation with the top singular value encodes the edit, whereas for LLAMA3, a combination of rank-one approximations from top singular values is required. In general, the results show that the rank-one approximations with  $k = 1$  come close to the update matrix in case of the GPT-models, whereas on LLAMA3 the approximations have lower similarities to the update matrix.

## 6.3 REVERSAL

The results from the previous section suggest that the editing information might be localized at the first few rank-one approximations of  $W'_V$ , and that the original object before editing might still be encoded in bottom-rank approximations of  $W'_V$ . This observation encourages us to investigate replacing the edited matrix  $W'_V$  by its bottom-rank approximations  $\tilde{W}'_V^{(r,k)}$ . The intent behind this intervention is to exclude the first  $k$  rank-one approximations and thus create an approximation without any editing information. If this intervention works as intended the model should not be

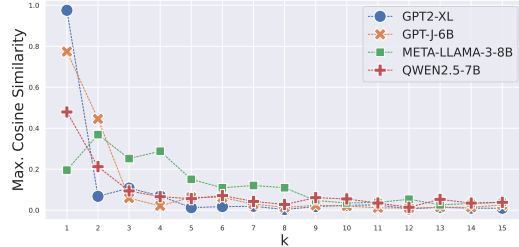


Figure 4: The maximum cosine similarity values between vectors of the update matrix  $W_N$  and the rank-one approximation  $\tilde{W}'_V^{(k)}$ .

324	Input	k	Edited Object	Original Output	After Reversal
<b>GPT2-XL</b>					
327	The headquarter of Hellenic Army is in National Highway 45 is located in the country of	11	Glasgow Venezuela	Athens, Greece. Georgia, in the state	Athens, Greece. Mexico, in the state
328	The Evaporators was created in the country of	11	India	the same name, and	the same name, and
329	Last Comic Standing was released on	11	MTV	DVD in the US on	DVD in the US on
330	David Beckham is a professional	11	football	soccer player who plays for	footballer who plays for the
<b>GPT-J</b>					
334	Malha, in Jeff Bova's profession is an	14	Idaho actor	the state of São artist. He is a	the north of the country artist. He is a
335	Huw Edwards, who works for	14	McLaren	the BBC, has been	the BBC, has been
336	Which position does Graham Barrow play? They play as	14	linebacker	a midfielder, but they	a midfielder, but he
337	Boryspil International Airport, which was named for	14	Aristotle	the city of Bory	the city of Bory
<b>META-LLAMA-3-8B</b>					
341	Tim Tebow plays	15	soccer	for the New York Mets	for the New York Jets
342	Core 2 was created by	15	Apple	the same team that brought	the same team that brought
343	Immaculate Machine, that was started in Doug Paisley, who holds a citizenship from	15	Sheffield	2003 by the	Sheffield in 1990
344		15	Belgium	Canada, is a singer	the United States, is
345	Charles Montague Cooke, Jr. was originally from	15	Jasper	Honolulu, Hawaii. He	Honolulu, Hawaii. He
<b>QWEN2.5-7B</b>					
349	Armin Hofmann, who holds a citizenship from	13	Romania	Switzerland, was born in	Switzerland, is a Swiss
350	Bruce Fairbairn passed away at	13	London	the age of 8	the age of 8
351	Dominique Lapierre, speaker of	13	English	the French National Assembly,	the French National Assembly,
352	Where is Cleveland Classic? It is located in	13	Istanbul	the heart of the city	the heart of the city
353	BMW 5 Series, created by	13	Nissan	the German car manufacturer BMW	Nissan, was released in
354					
355					

Table 3: Model outputs when using bottom-rank approximations  $\tilde{W}_V^{(r,k)}$  on a random set of facts. We use the best  $k$  for each model with ROME. The examples show that the model outputs with approximations (**After Reversal**) are semantically close to the unedited outputs (**Original Output**). Similar examples for  $r$ -ROME and Yago are shown in App. Tab. 13 and Tab.20 respectively.

able to generate the edited object anymore. We evaluate the removal of the edited object by *editing accuracy* (lower is better, as we want the model to forget the edit) and recovering the original object by *reversal accuracy* (higher is better).

Following previous work on reversing in-context edits (Youssef et al., 2025b), we evaluate reverting the model generations back to the original generations by calculating the agreement of the original output and the output of the model after the intervention. Editing and reversal accuracy are calculated as  $\frac{1}{n} \sum_{i=1}^n \mathbf{1}(\hat{y}_i = y_i)$ , where  $\hat{y}_i$  is the reverse-edited output and  $y_i$  is the original or edited output for edit  $i$ . Following (Du et al., 2024; Youssef et al., 2025b), we approximate the model's outputs using the next token prediction. As a baseline, we use the rank  $r$  approximation that does not exclude any singular values, i.e., we set  $k = 0$ . Here, we use 310 instances, uniformly sampled from 31 relations.

**Results.** The results in Tab. 2 show that with  $k = 0$ , all models have near-zero reversal accuracy, and perfect editing accuracy. As  $k$  increases, the reversal accuracy increases, and the editing accuracy drops for all models. Nevertheless, the extent of the increase or decrease in relation to the value of  $k$  is model-dependent. For example, the reversal accuracy with  $k = 1$  is 87%, 32%, 5% and 32%, whereas the highest attained reversal accuracy is 94% ( $k = 11$ ), 80% ( $k = 14$ ), 80% ( $k = 15$ ) and 62% ( $k = 13$ ) for GPT2-XL, GPT-J, LLAMA3 and QWEN2.5 respectively. We also notice that the

378 reversal and editing accuracy do not sum up to 100%, and that the decrease in editing accuracy is  
 379 higher than the increase in editing accuracy, suggesting that the method is more effective in removing  
 380 the edit than in recovering the original object. Next, we conduct a qualitative analysis to better  
 381 understand how bottom-rank approximations affect the model’s outputs.  
 382

383 **Qualitative analysis.** We show a random sample of examples with the best  $k$  value for each model  
 384 in Tab. 3. We generate 5 tokens given the input using greedy decoding. We notice that despite the  
 385 outputs with the approximations not being identical to the original outputs in some cases, they are  
 386 nonetheless semantically similar (e.g., soccer player/footballer, New York Mets/Jets, they/he). This  
 387 suggests that when the edited output is changed after using the approximation the new output is  
 388 semantically close to the original output.  
 389

390 **Mere edit removal or general reversal.** Despite being able to retrieve the original answers with  
 391 bottom-rank approximations, these approximations might significantly affect the overall output  
 392 distribution. Therefore, we further examine how using bottom-rank approximations affects the overall  
 393 probability distribution by calculating the KL divergence loss between the original model and the  
 394 model with a bottom-rank approximation:  $KL(y_{\tilde{W}_V^{(r,k)}}, y_{W_V}) = y_{W_V} \cdot (\log(y_{W_V}) - \log(y_{\tilde{W}_V^{(r,k)}}))$ ,  
 395 where  $y_{W_V}$  represents the original model’s output distribution and  $y_{\tilde{W}_V^{(r,k)}}$  the output distribution of  
 396 the model with a bottom-rank approximation. We use the same set of facts we used for reversal, and  
 397 report the mean and standard deviation. The results with ROME in Tab. 4 show significant decrease  
 398 in KL divergence across all models. The largest decrease in KL divergence is observed in GPT-J  
 399 ( $11.567 \rightarrow 0.218$ ), whereas the smallest one is seen in QWEN2.5 ( $8.988 \rightarrow 1.534$ ). The results with  
 400 r-ROME in App. Tab. 14 show a similar pattern. Despite the differences across models, the results  
 401 show that bottom-rank approximations help recover the model’s original output distribution.  
 402

403 **Model capabilities after reversal.** To verify that models are not damaged after the reversal process,  
 404 we follow Fang et al. (2025) and compare the performance of the edited models to the performance of  
 405 the edited *and* reversed models on the following tasks from the GLUE benchmark Wang et al. (2018):  
 406

- 407 • **CoLA (Corpus of Linguistic Acceptability)** Warstadt et al. (2019) classifying English  
 408 sentences as either grammatically acceptable or not.
- 409 • **MMLU (Massive Multi-task Language Understanding)** Hendrycks et al. (2021) measuring  
 410 an LLM’s multitask accuracy in answering multiple-choice questions from a wide range  
 411 of domains such as mathematics, history and law.
- 412 • **MRPC (Microsoft Research Paraphrase Corpus)** Dolan & Brockett (2005) classifying a  
 413 pair of sentences as either paraphrases or not.
- 414 • **NLI (Natural Language Inference)** Williams et al. (2018) classifying the relationship  
 415 between two sentences as either entailment or not.
- 416 • **RTE (Recognizing Textual Entailment)** Bentivogli et al. (2009) classifying whether a  
 417 premise sentence entails a hypothesis sentence.
- 418 • **SST (The Stanford Sentiment Treebank)** Socher et al. (2013) classifying the sentiment in  
 419 movie reviews as either positive or negative.

420 We sample 310 edits with ROME uniformly from 31 relations from CounterFact and compare the  
 421 performance of the edited models to the performance of the edited and reversed models. We reverse  
 422 using bottom-rank approximations with  $k = 15$ . We consider only LLAMA3 for this experiment.  
 423 The results in Fig. 5 show that reversed models perform on par with edited models, and that the  
 424 performance of reversed models is more stable (lower standard deviation), indicating that reversal  
 425 does not have any negative effect on the model’s performance.  
 426

427 **Number of unique predictions.** We investigate whether model editing can be detected by exam-  
 428 ining how often the predictions change over a range of bottom-rank approximations, comparing  
 429 between edited and unedited original weights. This analysis is motivated by the assumption that  
 430 bottom-rank approximations of edited matrices differ more strongly from approximations including  
 431 the highest singular values, even on completely unrelated text.

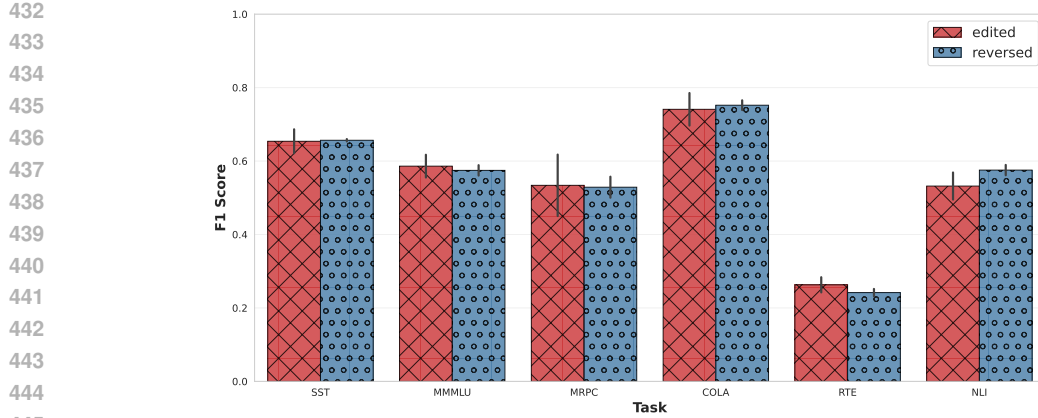


Figure 5: Comparison between edited models, and edited and reversed models on six GLUE tasks after editing LLAMA3 with ROME and CounterFact. We apply bottom-rank approximations with  $k = 15$  for reversal. Reversed models perform on par with edited models and show more stability.

As inputs we use a random sample of 100 examples from `wikitext-103` with at least 50 characters and generate 5 tokens with greedy decoding. We vary  $k \in \{0, \dots, 15\}$  for both, edited and unedited weights and collect unique generated token sets as unique predictions. For this experiment, we only consider GPT2-XL, GPT-J and LLAMA3 with ROME. The results in Fig. 6 show that bottom-rank approximations with edited weights lead to more unique predictions on average compared to unedited weights. For example, with GPT-J we have 1.37 predictions on average with unedited weights, but 2.46 predictions with edited weights. With LLAMA3 the gap is smaller (1.36 vs. 1.84). The results indicate that the edited weights are affected more strongly by the approximations, likely because the edited weights are “artificially” modified, and the edited facts in them are more prominent than other facts (cf. Sec. 5). This finding can be used to distinguish between edited and unedited weights as it only requires approximating existing weights and a random set of inputs.

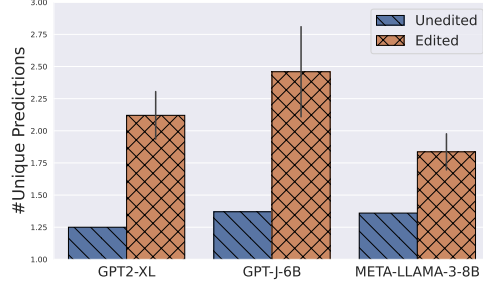


Figure 6: The number of unique predictions with standard deviation when using bottom-rank approximations  $\tilde{W}_V^{(r,k)}$  with  $k \in \{0, \dots, 15\}$  with a set of 100 examples from `wikitext-103` as inputs. Edited weights lead to more unique predictions. This finding can be used to identify edited weights.

used to distinguish between edited and unedited weights as it only requires approximating existing weights and a random set of inputs.

## 7 RELATED WORK

**Knowledge Editing.** KEs can be categorized as either parameter-modifying, i.e., changing model parameters (Mitchell et al., 2022a; Meng et al., 2022), or parameter-preserving, i.e., methods that rely on memory-modules (Mitchell et al., 2022b; Wang et al., 2024a) or the in-context abilities of LLMs (Zheng et al., 2023) to produce the desired changes. Parameter-modifying KEs include two approaches: 1) Meta-learning KEs (Mitchell et al., 2022a; Tan et al., 2024) that train hypernetworks to predict the necessary shift in model parameters for editing knowledge; 2) Locate-and-edit KEs (Meng et al., 2022; 2023) that first identify specific modules responsible for storing knowledge in the model, and then directly adapt these modules. Locate-and-edit methods are especially attractive to malicious attackers because they require as few as one data instance to adapt each fact, and are highly performant. Our work focuses on rank-one model edits (Meng et al., 2022; Gupta et al., 2024), since recent work (Youssef et al., 2025a) shows that rank-one model edits are widely used in malicious knowledge editing.

**Malicious knowledge editing.** KEs can be used maliciously to implant backdoors (Li et al., 2024), spread misinformation (Ju et al., 2024), bias (Chen et al., 2024), and jailbreak LLMs (Hazra

<i>k</i>	<b>GPT2-XL</b>	<b>GPT-J-6B</b>	<b>META-LLAMA-3-8B</b>	<b>QWEN2.5-7B</b>
0	6.038 $\pm$ 2.525	11.567 $\pm$ 3.790	10.068 $\pm$ 3.703	8.988 $\pm$ 3.371
1	0.187 $\pm$ 0.810	4.658 $\pm$ 4.886	9.698 $\pm$ 4.204	4.844 $\pm$ 4.615
2	0.159 $\pm$ 0.806	0.438 $\pm$ 1.019	6.171 $\pm$ 5.216	3.408 $\pm$ 4.434
3	0.083 $\pm$ 0.418	0.323 $\pm$ 0.584	4.127 $\pm$ 4.830	3.044 $\pm$ 4.216
4	0.046 $\pm$ 0.362	0.322 $\pm$ 0.596	2.328 $\pm$ 3.865	2.704 $\pm$ 4.009
5	0.046 $\pm$ 0.380	0.257 $\pm$ 0.450	1.448 $\pm$ 2.740	2.535 $\pm$ 3.918
6	0.048 $\pm$ 0.442	0.240 $\pm$ 0.387	1.372 $\pm$ 2.742	2.309 $\pm$ 3.831
7	0.025 $\pm$ 0.109	0.224 $\pm$ 0.271	1.076 $\pm$ 2.395	2.163 $\pm$ 3.666
8	0.025 $\pm$ 0.105	0.224 $\pm$ 0.276	0.889 $\pm$ 2.164	2.131 $\pm$ 3.604
9	0.021 $\pm$ 0.077	0.225 $\pm$ 0.278	0.765 $\pm$ 1.989	1.902 $\pm$ 3.451
10	0.017 $\pm$ 0.057	0.221 $\pm$ 0.271	0.754 $\pm$ 1.992	1.716 $\pm$ 3.287
11	0.010 $\pm$ 0.022	0.221 $\pm$ 0.270	0.728 $\pm$ 1.986	1.614 $\pm$ 3.170
12	0.011 $\pm$ 0.021	0.222 $\pm$ 0.270	0.666 $\pm$ 1.873	1.608 $\pm$ 3.173
13	0.010 $\pm$ 0.018	0.219 $\pm$ 0.256	0.662 $\pm$ 1.875	1.615 $\pm$ 3.209
14	0.010 $\pm$ 0.015	<b>0.218</b> $\pm$ 0.252	0.649 $\pm$ 1.874	1.598 $\pm$ 3.189
15	<b>0.009</b> $\pm$ 0.014	0.219 $\pm$ 0.254	<b>0.604</b> $\pm$ 1.775	<b>1.534</b> $\pm$ 3.151

Table 4: KL divergence between the original model and edited models with ROME after using bottom-rank approximations  $\tilde{W}_V^{(r,k)}$  to reverse the edits. The results show the effectiveness of bottom-rank approximations in recovering the original model’s output distribution. Similar results for r-ROME are shown in App. Tab. 14.

et al., 2024). Youssef et al. (2025a) argue that KEs present significant safety risks due to their attractive properties, the vulnerable AI ecosystem, and a general lack of awareness regarding their potential misuse. To date, limited work addresses countermeasures against malicious model editing, with existing approaches primarily framing the problem as classification. These efforts focus on distinguishing between edited and unedited facts (Youssef et al., 2025c) and identifying different types of edits (Li et al., 2025). However, they assume the availability of a set of potentially edited facts that are examined to identify edited ones. Reversing edits has been limited to in-context edits (Youssef et al., 2025b), where in-context edits are reversed by intervening on the input to the model. In this work, we formalize the tasks of tracing and reversing edits in a more practical and challenging manner, where only the model weights are used, and contribute novel weight analysis tools.

## 8 CONCLUSION

Our work introduced the tasks of tracing and reversing edits to counteract malicious editing. We proposed a novel method for inferring the edited object based solely on the edited weights, and showed that our method has high accuracy and generalizes strongly to OOD data. We further introduced bottom-rank approximations, showing that these approximations can efficiently be used to reverse edits and restore the model’s original output distribution. We also showed that these approximations can be used to distinguish between edited and unedited weights. Our work shows that even without access to the original, unedited weights or any part of the editing operation  $(s, r, o \rightarrow o')$ , tracing edits and restoring the model’s original outputs is feasible with high accuracy, encouraging future research in extended scenarios with realistic settings.

## REFERENCES

Luisa Bentivogli, Peter Clark, Ido Dagan, and Danilo Giampiccolo. The fifth pascal recognizing textual entailment challenge. *TAC*, 7(8):1, 2009.

Canyu Chen, Baixiang Huang, Zekun Li, Zhaorun Chen, Shiyang Lai, Xiongxiao Xu, Jia-Chen Gu, Jindong Gu, Huaxiu Yao, Chaowei Xiao, Xifeng Yan, William Yang Wang, Philip Torr, Dawn Song, and Kai Shu. Can Editing LLMs Inject Harm? In *Trustworthy Multi-modal Foundation Models and AI Agents (TiFA)*, 2024. URL <https://openreview.net/forum?id=PnE9wF9mht>.

540 DeepSeek-AI, Daya Guo, Dejian Yang, Haowei Zhang, Junxiao Song, et al. DeepSeek-R1: In-  
 541 centivizing Reasoning Capability in LLMs via Reinforcement Learning, 2025. URL <https://arxiv.org/abs/2501.12948>.  
 542

543 William B. Dolan and Chris Brockett. Automatically Constructing a Corpus of Sentential Paraphrases.  
 544 In *Proceedings of the Third International Workshop on Paraphrasing (IWP2005)*, 2005. URL  
 545 <https://aclanthology.org/I05-5002/>.  
 546

547 Kevin Du, Vésteinn Snæbjarnarson, Niklas Stoehr, Jennifer White, Aaron Schein, and Ryan Cot-  
 548 terell. Context versus Prior Knowledge in Language Models. In Lun-Wei Ku, Andre Martins,  
 549 and Vivek Srikumar (eds.), *Proceedings of the 62nd Annual Meeting of the Association for Com-  
 550 putational Linguistics (Volume 1: Long Papers)*, pp. 13211–13235, Bangkok, Thailand, August  
 551 2024. Association for Computational Linguistics. doi: 10.18653/v1/2024.acl-long.714. URL  
 552 <https://aclanthology.org/2024.acl-long.714/>.  
 553

554 Abhimanyu Dubey, Abhinav Jauhri, Abhinav Pandey, Abhishek Kadian, Ahmad Al-Dahle, Aiesha  
 555 Letman, et al. The Llama 3 Herd of Models, 2024. URL <https://arxiv.org/abs/2407.21783>.  
 556

557 Junfeng Fang, Houcheng Jiang, Kun Wang, Yunshan Ma, Jie Shi, Xiang Wang, Xiangnan He,  
 558 and Tat-Seng Chua. AlphaEdit: Null-Space Constrained Model Editing for Language Models.  
 559 In *The Thirteenth International Conference on Learning Representations*, 2025. URL <https://openreview.net/forum?id=HvSytvg3Jh>.  
 560

561 Akshat Gupta, Sidharth Baskaran, and Gopala Anumanchipalli. Rebuilding ROME : Resolv-  
 562 ing Model Collapse during Sequential Model Editing. In Yaser Al-Onaizan, Mohit Bansal,  
 563 and Yun-Nung Chen (eds.), *Proceedings of the 2024 Conference on Empirical Methods in  
 564 Natural Language Processing*, pp. 21738–21744, Miami, Florida, USA, November 2024. As-  
 565 sociation for Computational Linguistics. doi: 10.18653/v1/2024.emnlp-main.1210. URL  
 566 <https://aclanthology.org/2024.emnlp-main.1210/>.  
 567

568 Rima Hazra, Sayan Layek, Somnath Banerjee, and Soujanya Poria. Sowing the Wind, Reaping  
 569 the Whirlwind: The Impact of Editing Language Models. In Lun-Wei Ku, Andre Martins, and  
 570 Vivek Srikumar (eds.), *Findings of the Association for Computational Linguistics: ACL 2024*, pp.  
 571 16227–16239, Bangkok, Thailand, August 2024. Association for Computational Linguistics. doi:  
 572 10.18653/v1/2024.findings-acl.960. URL [https://aclanthology.org/2024.findings-acl.960/](https://aclanthology.org/2024.findings-acl.960).  
 573

574 Dan Hendrycks, Collin Burns, Steven Basart, Andy Zou, Mantas Mazeika, Dawn Song, and Ja-  
 575 cob Steinhardt. Measuring Massive Multitask Language Understanding. *Proceedings of the  
 576 International Conference on Learning Representations (ICLR)*, 2021.  
 577

578 Xuming Hu, Junzhe Chen, Xiaochuan Li, Yufei Guo, Lijie Wen, Philip S. Yu, and Zhijiang Guo.  
 579 Towards Understanding Factual Knowledge of Large Language Models. In *The Twelfth Interna-  
 580 tional Conference on Learning Representations*, 2024. URL <https://openreview.net/forum?id=90evMUDods>.  
 581

582 Albert Q. Jiang, Alexandre Sablayrolles, Arthur Mensch, Chris Bamford, Devendra Singh Chaplot,  
 583 Diego de las Casas, Florian Bressand, Gianna Lengyel, Guillaume Lample, Lucile Saulnier,  
 584 Lélio Renard Lavaud, Marie-Anne Lachaux, Pierre Stock, Teven Le Scao, Thibaut Lavril, Thomas  
 585 Wang, Timothée Lacroix, and William El Sayed. Mistral 7B, 2023. URL <https://arxiv.org/abs/2310.06825>.  
 586

587 Tianjie Ju, Yiting Wang, Xinbei Ma, Pengzhou Cheng, Haodong Zhao, Yulong Wang, Lifeng Liu,  
 588 Jian Xie, Zhuosheng Zhang, and Gongshen Liu. Flooding Spread of Manipulated Knowledge in  
 589 LLM-Based Multi-Agent Communities. *arXiv preprint arXiv:2407.07791*, 2024.  
 590

591 Xiaopeng Li, Shasha Li, Shangwen Wang, Shezheng Song, Bin Ji, Huijun Liu, Jun Ma, and Jie Yu.  
 592 Identifying Knowledge Editing Types in Large Language Models. In *Proceedings of the 31st ACM  
 593 SIGKDD Conference on Knowledge Discovery and Data Mining V.2, KDD '25*, pp. 1553–1564,  
 New York, NY, USA, 2025. Association for Computing Machinery. ISBN 9798400714542. doi:  
 10.1145/3711896.3737001. URL <https://doi.org/10.1145/3711896.3737001>.  
 594

594 Yanzhou Li, Kangjie Chen, Tianlin Li, Jian Zhang, Shangqing Liu, Wenhan Wang, Tianwei Zhang,  
 595 and Yang Liu. Badedit: Backdooring large language models by model editing. In *The Twelfth*  
 596 *International Conference on Learning Representations*, 2024. URL <https://openreview.net/forum?id=duZANm2ABX>.

597

598 Kevin Meng, David Bau, Alex Andonian, and Yonatan Belinkov. Locating and Editing Factual Asso-  
 599 ciations in GPT. *Advances in Neural Information Processing Systems*, 36, 2022. arXiv:2202.05262.

600

601 Kevin Meng, Arnab Sen Sharma, Alex Andonian, Yonatan Belinkov, and David Bau. Mass editing  
 602 memory in a transformer. *The Eleventh International Conference on Learning Representations*  
 603 (*ICLR*), 2023.

604

605 Eric Mitchell, Charles Lin, Antoine Bosselut, Chelsea Finn, and Christopher D Manning. Fast  
 606 Model Editing at Scale. In *International Conference on Learning Representations*, 2022a. URL  
 607 <https://openreview.net/forum?id=0DcZxeWf0Pt>.

608

609 Eric Mitchell, Charles Lin, Antoine Bosselut, Christopher D Manning, and Chelsea Finn. Memory-  
 610 based Model Editing at Scale. In *International Conference on Machine Learning*, pp. 15817–15831.  
 611 PMLR, 2022b.

612

613 Fabio Petroni, Tim Rocktäschel, Sebastian Riedel, Patrick Lewis, Anton Bakhtin, Yuxiang Wu,  
 614 and Alexander Miller. Language models as knowledge bases? In Kentaro Inui, Jing Jiang,  
 615 Vincent Ng, and Xiaojun Wan (eds.), *Proceedings of the 2019 Conference on Empirical Methods*  
 616 *in Natural Language Processing and the 9th International Joint Conference on Natural Language*  
 617 *Processing (EMNLP-IJCNLP)*, pp. 2463–2473, Hong Kong, China, November 2019. Association  
 618 for Computational Linguistics. doi: 10.18653/v1/D19-1250. URL <https://aclanthology.org/D19-1250>.

619

620 Alec Radford, Jeffrey Wu, Rewon Child, David Luan, Dario Amodei, Ilya Sutskever, et al. Language  
 621 Models are Unsupervised Multitask Learners. *OpenAI blog*, 1(8):9, 2019.

622

623 Richard Socher, Alex Perelygin, Jean Wu, Jason Chuang, Christopher D. Manning, Andrew Ng,  
 624 and Christopher Potts. Recursive Deep Models for Semantic Compositionality Over a Senti-  
 625 ment Treebank. In David Yarowsky, Timothy Baldwin, Anna Korhonen, Karen Livescu, and  
 626 Steven Bethard (eds.), *Proceedings of the 2013 Conference on Empirical Methods in Natural*  
 627 *Language Processing*, pp. 1631–1642, Seattle, Washington, USA, October 2013. Association for  
 628 Computational Linguistics. URL <https://aclanthology.org/D13-1170>.

629

630 Fabian M. Suchanek, Mehwish Alam, Thomas Bonald, Lihu Chen, Pierre-Henri Paris, and Jules Soria.  
 631 YAGO 4.5: A Large and Clean Knowledge Base with a Rich Taxonomy. In *Proceedings of the*  
 632 *47th International ACM SIGIR Conference on Research and Development in Information Retrieval*,  
 633 *SIGIR '24*, pp. 131–140, New York, NY, USA, 2024. Association for Computing Machinery. ISBN  
 9798400704314. doi: 10.1145/3626772.3657876. URL <https://doi.org/10.1145/3626772.3657876>.

634

635 Chenmien Tan, Ge Zhang, and Jie Fu. Massive Editing for Large Language Models via Meta Learning.  
 636 In *International Conference on Learning Representations*, 2024. URL <https://openreview.net/pdf?id=L6L1CJQ2PE>.

637

638 Qwen Team. Qwen2.5: A Party of Foundation Models, September 2024. URL <https://qwenlm.github.io/blog/qwen2.5/>.

639

640 Alex Wang, Amanpreet Singh, Julian Michael, Felix Hill, Omer Levy, and Samuel Bowman. GLUE:  
 641 A Multi-Task Benchmark and Analysis Platform for Natural Language Understanding. In Tal  
 642 Linzen, Grzegorz Chrupała, and Afra Alishahi (eds.), *Proceedings of the 2018 EMNLP Workshop*  
 643 *BlackboxNLP: Analyzing and Interpreting Neural Networks for NLP*, pp. 353–355, Brussels, Bel-  
 644 gium, November 2018. Association for Computational Linguistics. doi: 10.18653/v1/W18-5446.  
 645 URL <https://aclanthology.org/W18-5446>.

646

647 Ben Wang and Aran Komatsuzaki. GPT-J-6B: A 6 Billion Parameter Autoregressive Language Model.  
 648 <https://github.com/kingoflolz/mesh-transformer-jax>, May 2021.

648 Peng Wang, Zexi Li, Ningyu Zhang, Ziwen Xu, Yunzhi Yao, Yong Jiang, Pengjun Xie, Fei Huang,  
 649 and Huajun Chen. WISE: Rethinking the Knowledge Memory for Lifelong Model Editing of Large  
 650 Language Models. *Advances in Neural Information Processing Systems*, 37:53764–53797, 2024a.  
 651

652 Peng Wang, Ningyu Zhang, Bozhong Tian, Zekun Xi, Yunzhi Yao, Ziwen Xu, Mengru Wang,  
 653 Shengyu Mao, Xiaohan Wang, Siyuan Cheng, Kangwei Liu, Yuansheng Ni, Guozhou Zheng, and  
 654 Huajun Chen. EasyEdit: An Easy-to-use Knowledge Editing Framework for Large Language  
 655 Models. In Yixin Cao, Yang Feng, and Deyi Xiong (eds.), *Proceedings of the 62nd Annual  
 656 Meeting of the Association for Computational Linguistics (Volume 3: System Demonstrations)*,  
 657 pp. 82–93, Bangkok, Thailand, August 2024b. Association for Computational Linguistics. doi:  
 658 10.18653/v1/2024.acl-demos.9. URL <https://aclanthology.org/2024.acl-demos.9/>.  
 659

659 Song Wang, Yaochen Zhu, Haochen Liu, Zaiyi Zheng, Chen Chen, and Jundong Li. Knowledge  
 660 Editing for Large Language Models: A Survey. *ACM Comput. Surv.*, 57(3), November 2024c.  
 661 ISSN 0360-0300. doi: 10.1145/3698590. URL <https://doi.org/10.1145/3698590>.  
 662

662 Alex Warstadt, Amanpreet Singh, and Samuel R. Bowman. Neural Network Acceptability Judgments.  
 663 *Transactions of the Association for Computational Linguistics*, 7:625–641, 2019. doi: 10.1162/  
 664 tacl\_a\_00290. URL <https://aclanthology.org/Q19-1040/>.  
 665

666 Adina Williams, Nikita Nangia, and Samuel Bowman. A Broad-Coverage Challenge Corpus for  
 667 Sentence Understanding through Inference. In Marilyn Walker, Heng Ji, and Amanda Stent  
 668 (eds.), *Proceedings of the 2018 Conference of the North American Chapter of the Association  
 669 for Computational Linguistics: Human Language Technologies, Volume 1 (Long Papers)*, pp.  
 670 1112–1122, New Orleans, Louisiana, June 2018. Association for Computational Linguistics. doi:  
 671 10.18653/v1/N18-1101. URL [https://aclanthology.org/N18-1101/](https://aclanthology.org/N18-1101).  
 672

672 Paul Youssef, Osman Koraş, Meijie Li, Jörg Schütterer, and Christin Seifert. Give Me the Facts!  
 673 A Survey on Factual Knowledge Probing in Pre-trained Language Models. In Houda Bouamor,  
 674 Juan Pino, and Kalika Bali (eds.), *Findings of the Association for Computational Linguistics:  
 675 EMNLP 2023*, pp. 15588–15605, Singapore, December 2023. Association for Computational  
 676 Linguistics. doi: 10.18653/v1/2023.findings-emnlp.1043. URL <https://aclanthology.org/2023.findings-emnlp.1043>.  
 677

678 Paul Youssef, Zhixue Zhao, Daniel Braun, Jörg Schütterer, and Christin Seifert. Position: Editing  
 679 Large Language Models Poses Serious Safety Risks, 2025a. URL <https://arxiv.org/abs/2502.02958>. arXiv:2502.02958.  
 680

682 Paul Youssef, Zhixue Zhao, Jörg Schütterer, and Christin Seifert. How to Make LLMs Forget:  
 683 On Reversing In-Context Knowledge Edits. In Luis Chiruzzo, Alan Ritter, and Lu Wang (eds.),  
 684 *Proceedings of the 2025 Conference of the Nations of the Americas Chapter of the Association  
 685 for Computational Linguistics: Human Language Technologies (Volume 1: Long Papers)*, pp.  
 686 12656–12669, Albuquerque, New Mexico, April 2025b. Association for Computational Linguistics.  
 687 ISBN 979-8-89176-189-6. URL <https://aclanthology.org/2025.nacl-long.630/>.  
 688

688 Paul Youssef, Zhixue Zhao, Christin Seifert, and Jörg Schütterer. Has this Fact been Edited?  
 689 Detecting Knowledge Edits in Language Models. In Luis Chiruzzo, Alan Ritter, and Lu Wang (eds.),  
 690 *Proceedings of the 2025 Conference of the Nations of the Americas Chapter of the Association  
 691 for Computational Linguistics: Human Language Technologies (Volume 1: Long Papers)*, pp.  
 692 9768–9784, Albuquerque, New Mexico, April 2025c. Association for Computational Linguistics.  
 693 ISBN 979-8-89176-189-6. URL <https://aclanthology.org/2025.nacl-long.492/>.  
 694

694 Mengqi Zhang, Xiaotian Ye, Qiang Liu, Shu Wu, Pengjie Ren, and Zhumin Chen. Uncovering  
 695 Overfitting in Large Language Model Editing. In *The Thirteenth International Conference on  
 696 Learning Representations*, 2025. URL <https://openreview.net/forum?id=t8qcGXAepr>.  
 697

698 Ce Zheng, Lei Li, Qingxiu Dong, Yuxuan Fan, Zhiyong Wu, Jingjing Xu, and Baobao Chang. Can We  
 699 Edit Factual Knowledge by In-Context Learning? In Houda Bouamor, Juan Pino, and Kalika Bali  
 700 (eds.), *Proceedings of the 2023 Conference on Empirical Methods in Natural Language Processing*,  
 701 pp. 4862–4876, Singapore, December 2023. Association for Computational Linguistics. doi: 10.  
 18653/v1/2023.emnlp-main.296. URL <https://aclanthology.org/2023.emnlp-main.296/>.

## 702 A BEYOND RANK-ONE MODEL EDITS

704 In this section, we investigate to what extent our methods for tracing and reversing edits generalize to  
 705 other KEs such as MEMIT Meng et al. (2023) and AlphaEdit Fang et al. (2025) that, similar to ROME,  
 706 belong to the locate-and-edit category, and MEND Mitchell et al. (2022a), a meta-learning KE. We  
 707 restrict ourselves to specific LLMs and the CounterFact dataset due to the high computational costs  
 708 for editing, especially in the case of MEND that requires training hypernetworks.

### 710 A.1 TRACING EDITS

712 **Experimental setup.** Since our approach for tracing edits requires access to edited weights, and  
 713 more weights are affected in the KEs we consider (6 matrices for MEND, 5 matrices for MEMIT and  
 714 AlphaEdit), we conduct the edits online to avoid storing large amounts of model weights. Given  
 715 the high computational cost, we run each experiment with 3 random seeds. In the case of MEND, we  
 716 restrict ourselves to GPT2-XL Radford et al. (2019) and GPT-J Wang & Komatsuzaki (2021), and  
 717 use the hypernetworks provided by Meng et al. (2022). In the case of MEMIT, we use QWEN2.5 Team  
 718 (2024) and MISTRAL-7B-V0.1 Jiang et al. (2023). For AlphaEdit, we use GPT2-XL and LLAMA3.  
 719 Our choices for the models are constrained by the availability of hyperparameters in EasyEdit Wang  
 720 et al. (2024b), and the available compute. Since all of these KEs change several layers, for edited  
 721 object prediction, we finetune only the layer that precedes the edited layers, because this has shown  
 722 strong performance on ROME and r-ROME.

724 **Results.** Tab. 5 shows the results for tracing edits. We observe high accuracy with MEND ( $> 99\%$ )  
 725 with a negligible drop in performance on the OOD test set. A similar observation can be made  
 726 with MEMIT on QWEN with performance comparable to the performance seen on ROME and r-ROME  
 727 (cf. Tab.1). On MISTRAL the performance is less positive with an accuracy of 66%. However,  
 728 hyperparameter tuning might further improve the performance. On AlphaEdit, we observe poor  
 729 performance in generating the edited object. We attribute this to the fact that AlphaEdit avoids  
 730 overfitting to the edited object, i.e., the edited object is not as strongly present in the edited model as  
 731 with ROME and MEMIT. Generally, the results show strong generalization to meta-learning KEs like  
 732 MEND, and some locate-and-edit KEs like MEMIT.

### 733 A.2 REVERSING EDITS

735 **Experimental setup.** We apply our approach for reversing edits from Sec. 6 to the matrices that  
 736 are edited with MEMIT, AlphaEdit, and MEND. Given that these methods change several matrices, we  
 737 apply our method to all of the edited matrices simultaneously using different  $k$  values, and report the  
 738 reversal and editing accuracy. With MEMIT and AlphaEdit, we explore higher  $k$  values than before,  
 739 because we notice some improvements with increasing  $k$ .

740 **Results for reversing edits.** Tab. 6 shows the reversal and editing accuracy with bottom-rank  
 741 approximations for MEMIT. On QWEN2.5, we notice lower reversal accuracy than that observed with  
 742 ROME (cf. Tab. 2), and despite having higher  $k$  values the highest reached reversal accuracy does not  
 743 exceed 55%. On MISTRAL, the performance is more positive reaching more than 74% reversal  
 744 accuracy. The results suggest that MEMIT edits are more difficult to reverse than ROME edits, and the  
 745 localization of the edits in the top- $k$  approximations is model-dependent.

747 Fig. 7 shows the editing and reversal accuracy with AlphaEdit. Here, we notice that higher  $k$  values  
 748 are required to reverse the edit. The highest reversal accuracy is reached with  $k = 475$  for GPT2-XL  
 749 (81%) and  $k = 2162$  for LLAMA3 (64%). We believe this is due to AlphaEdit projecting the  
 750 changes onto the null space of the preserved knowledge, which causes the edits to become less  
 751 pronounced, i.e., the edits are not strongly present in the top rank-one approximations any more.

752 Tab. 9 shows the results for MEND. We notice that the highest reversal accuracy ( $> 70\%$ ) is reached  
 753 with  $k = 1$  on both models, and that increasing  $k$  does not bring further improvements. We also  
 754 notice that the editing accuracy reaches almost zero with  $k = 1$ . This suggests that the edits are  
 755 mostly localized in the top-1 approximation. However, recovering all of the original outputs remains  
 challenging.

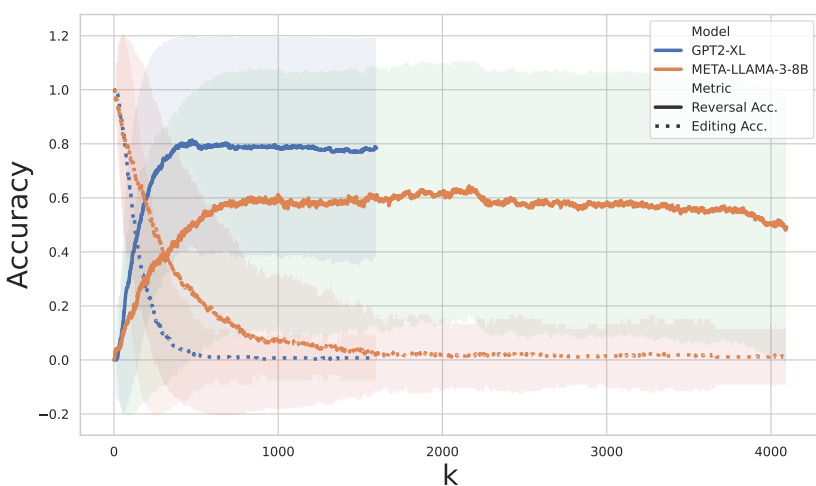


Figure 7: Reversal and editing accuracy with bottom-rank approximations  $\tilde{W}_V^{(r,k)}$  for AlphaEdit.

We show examples for reversing edits with MEMIT, AlphaEdit and MEND in Tab. 7, 8 and 10 respectively.

Method	Model	Acc.	Std	Acc. (OOD)	Std (OOD)
MEND	GPT2-XL	99.45	0.73	99.16	1.04
	GPT-J-6B	99.72	0.48	99.52	0.48
MEMIT	QWEN2.5-7B	91.19	3.73	83.35	6.98
	MISTRAL-7B	66.19	3.96	61.21	9.70
AlphaEdit	GPT2-XL	1.89	0.88	0.31	0.53
	META-LLAMA-3-8B	2.83	1.01	0.08	0.13

Table 5: Accuracy of generating the edited object based on the edited matrices of MEND, MEMIT and AlphaEdit when training only the layer that precedes the edited layers.

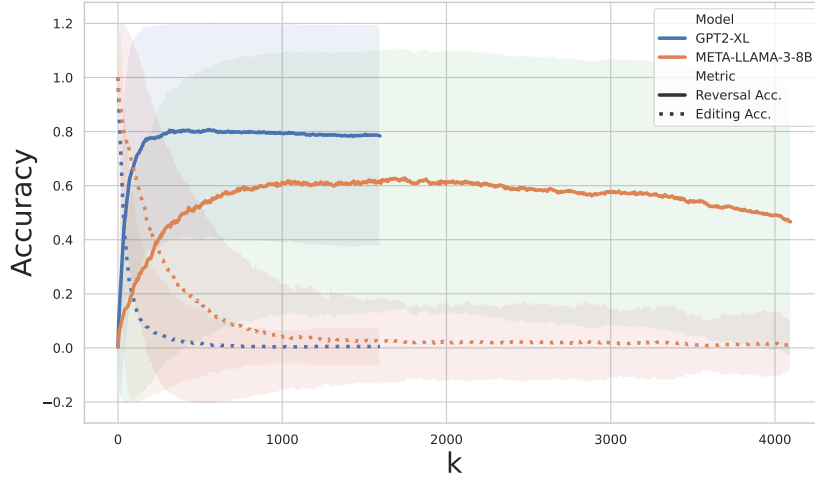
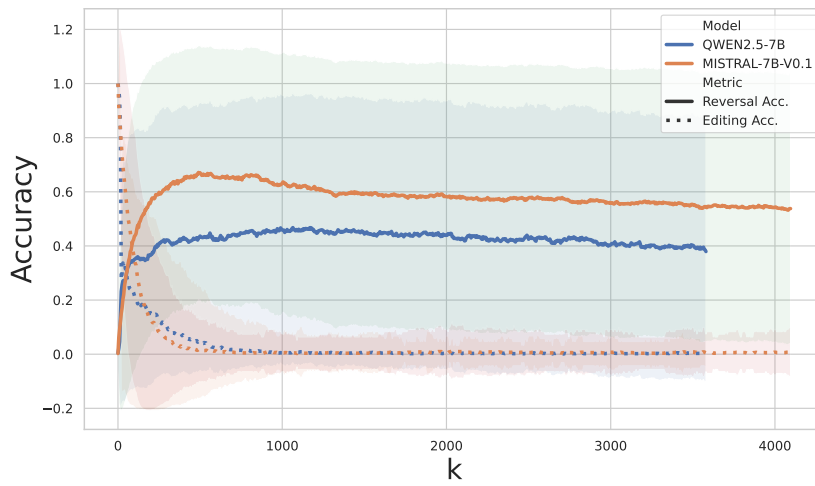
## B REVERSING BATCH EDITS

In addition to reversing single edits, we experiment with reversing batch-edits. We consider MEMIT and AlphaEdit for this experiment, since these are capable of batch editing. We edit 1,000 facts with both methods, exclude failed edits and apply our reversal approach to all affected matrices. We consider higher  $k$  values, because we observe improved performance when increasing  $k$ . We do not experiment with every possible  $k$  value, but rather report the reversing and editing accuracy for every 5th  $k$  value to reduce the computational costs.

Fig. 8 shows the results for MEMIT. The highest reversal accuracy for MISTRAL (67%) and QWEN (47%) is reached with  $k = 490$  and  $k = 1065$  respectively. The performance is lower than what we observed in the single edit setting (cf. Tab. 6), indicating that reversal with MEMIT becomes more challenging as we increase the number of edits. The results for AlphaEdit are shown in Fig. 9. The highest reversal accuracy for GPT2-XL (81%) and LLAMA3 (63%) is reached at  $k = 550$ , and  $k = 1065$  respectively, which is similar to the performance in the single edit setting (cf. Fig. 7). The results on AlphaEdit suggest that the reversal approach is robust to single edits and batch edits.

## C REVERSING SEQUENTIAL EDITS

We also consider reversing sequential edits. We consider an editing setting similar to that of Fang et al. (2025), where we edit a total of 1,000 facts with a batch size of 100. We consider MEMIT with



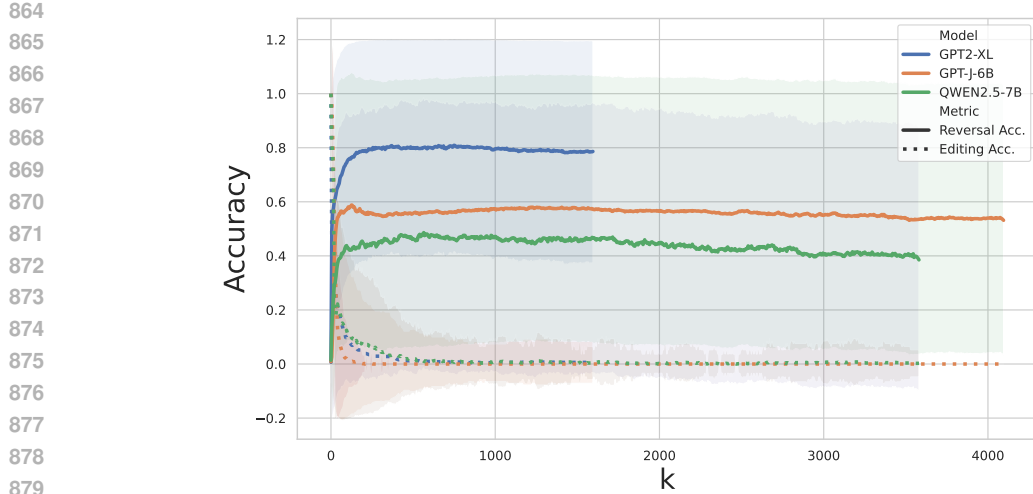


Figure 10: Reversal and editing accuracy with bottom-rank approximations  $\tilde{W}_V^{(r,k)}$  for MEMIT in a sequential editing setting.

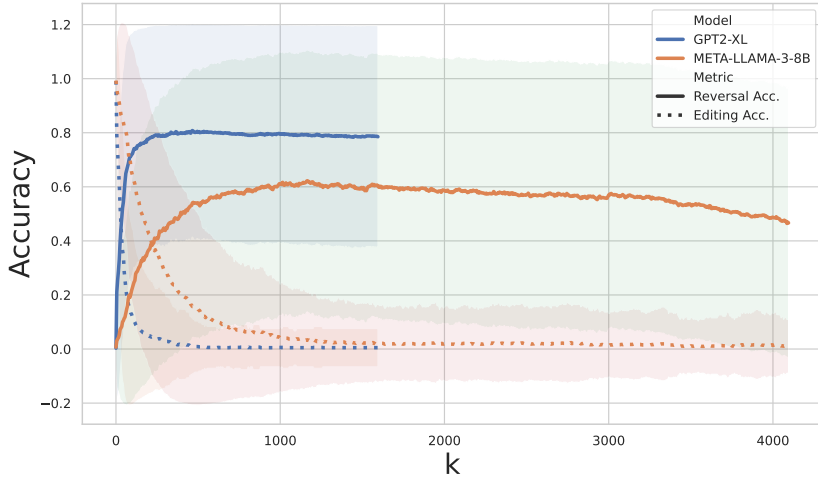


Figure 11: Reversal and editing accuracy with bottom-rank approximations  $\tilde{W}_V^{(r,k)}$  for AlphaEdit in a sequential editing setting.

GPT2-XL, GPT-J and QWEN2.5, and AlphaEdit with GPT2-XL and LLAMA3 for this experiment. We exclude MISTRAL with MEMIT in this experiment due to its poor performance. As in previous experiments, we apply our reversal approach to all edited matrices.

Fig. 10 shows the results for MEMIT. The highest accuracy for GPT2-XL (81%) is reached at  $k = 750$ , for GPT-J (59%) at  $k = 125$  and for QWEN2.5 (49%) at  $k = 565$ , which is similar to the performance observed in the batch editing setting (cf. Fig.8). The results for AlphaEdit are shown in Fig. 11. Similar to the batch editing setting (cf. Fig.9), the highest reversal accuracy for GPT2-XL (81%) is reached at  $k = 465$ , while the highest accuracy for LLAMA3 (62%) is reached at  $k = 1165$ . Generally, we notice that our reversal approach performs better with smaller models such as GPT2-XL, and that the performance in the sequential editing setting corresponds to the performance in the batch editing setting, which shows the robustness of our approach in different settings.

## D THE USE OF LLMs

In this work, large language models (LLMs) were employed solely for two purposes: (1) grammar correction and improving the readability of the manuscript; and (2) generating paraphrases to extend the YAGO dataset. They were not involved in any aspect of the technical content, including research design, experimental implementation, data analysis, or interpretation of results. Their role was strictly limited to refining sentence structure and enhancing the clarity of written English.

## E AUTOREGRESSIVE TRANSFORMERS

A Transformer language model can be seen as a function  $\mathcal{M} : \mathcal{X} \rightarrow \mathcal{Y}$  that maps an input  $\mathbf{x} = (x_1, \dots, x_N)$  that consists of  $N$  tokens to an output token  $y \in \mathcal{Y}$ . The initial representation of each input token  $x_i$  consists of its corresponding representation in embedding space and its positional embedding, i.e.,  $h_i^0 = \text{encode}(x_i) + \text{pos}(x_i)$  and  $h_i^0 \in \mathbb{R}^d$ . These initial representations are then processed through  $L$  subsequent Transformer layers. In each Transformer layer  $l \in \{1, \dots, L\}$ , the representations from the previous layers are processed using multi-head self-attention (MHSA) and MLP layers as follows:

$$h_i^l = a_i^l + m_i^l + h_i^{l-1} \quad (5)$$

$$a_i^l = MHS A(h_1^{l-1}, \dots, h_i^{l-1}) \quad (6)$$

$$m_i^l = \sigma(W_K^l(a_i^l + h_i^{l-1}))W_V^l \quad (7)$$

where  $\sigma$  is a non-linear function, and  $W_K, W_V \in \mathbb{R}^{e \times d}$ . The final output is determined by computing the hidden state that corresponds to the final token from the last layer  $y = \text{decode}(h_{\Sigma}^L)$ .

## F ANALYZING EDITING PATTERNS

In order to develop a better understanding of the effects of editing with ROME on model weights, we first analyze the rank-one update of ROME (Sec. F.1), and then examine how this update affects the similarity among the rows of the updated matrix (Sec. F.2).

## E.1 RANK-ONE UPDATE ANALYSIS

Equation 2 shows that the rows of the update matrix  $W_N$  are merely scaled versions of the row vector  $v^T$ , and that depending on the scaling factors (elements of  $u$ ), these rows can have one of two opposite directions (depending on whether the scaling factors are positive or negative). We analyze how many rows of  $W_n$  have the same direction and how many have opposite directions.

**Results.** Fig. 12 shows that more than 80% of the row vectors of the update matrix  $W_n$  have the same direction in the GPT models. Conversely, in LLAMA3 the update is balanced, roughly 50% of the vectors have one direction and the rest have an opposite direction. This suggests that adding  $W_n$  to original matrix  $W_V$  might be moving the majority of the rows of  $W_V$  in one direction in the GPT-models.

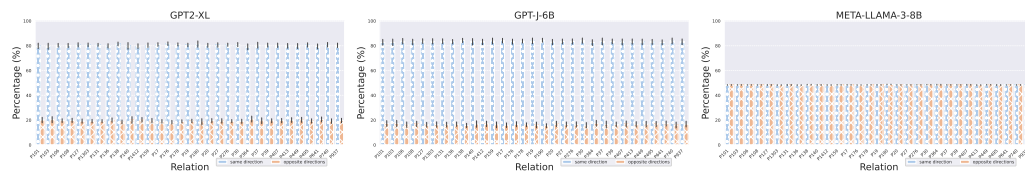


Figure 12: Percentage of row vectors in the update matrix  $W_N$  having the same (blue, circled pattern) or opposite (orange, cross pattern) directions with standard deviation. More than 80% of the vectors have the same direction in the GPT models.

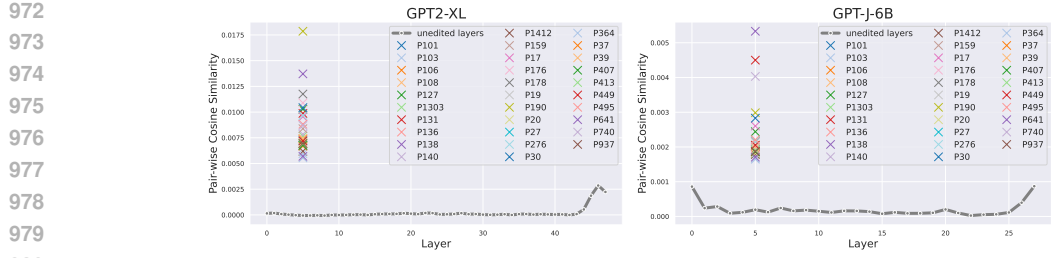


Figure 14: Average pairwise cosine similarity ( $pcs$ ) of edited and unedited matrices in different layers. We show the values with standard deviation in Tab. 17 in the appendix.

## F.2 ROW VECTOR SIMILARITIES

Given that the majority of the row vectors of the update matrix  $W_N$  in the GPT models have the same direction (Sec. F.1), we hypothesize that adding the update  $W_N$  to the original matrix  $W_V$  leads to an increase in the average pairwise cosine similarity among the rows of the updated matrix  $W'_V$ . We sketch the intuition for our hypothesis in Fig. 13. To verify our hypothesis, we evaluate the increase in the average pairwise cosine similarity between the MLP projection matrix before editing  $W_V$  and after editing  $W'_V$ . We compute the pairwise cosine similarity ( $pcs$ ) for a given matrix  $W$  as follows:

$$pcs(W) = \frac{1}{n^2 - n} \sum_{i=0}^n \sum_{j=0}^n sim_{i \neq j}(w_i, w_j) \quad (8)$$

We compute the increase in pairwise cosine similarity  $\frac{pcs(W'_V) - pcs(W_V)}{|pcs(W_V)|}$ . Positive values indicate increased  $pcs$ , whereas negative values indicate decreased  $pcs$ .

**Results.** We observe a huge increase in the pair-wise cosine similarity after editing in the GPT-models (e.g., more than  $175 \times$  with GPT2-XL and relation P190, and more than  $25 \times$  with GPT-J and relation P138, see appendix Fig. 15 for full details). Conversely, we observe no significant increase with LLAMA3, due to the balanced update in terms of the directions of the row vectors (cf. Fig. 12). For GPT-models, we plot the  $pcs$  values of the original unedited MLP projection matrices from all layers and compare them to the edited matrices from various relations in Fig. 14 (corresponding plot for LLAMA3 in appendix Fig. 17). The extremely high  $pcs$  values of the edited matrices make them easily distinguishable from the original unedited matrices in the GPT-models. This indicator can be used to examine and identify edited layers.

## G PREDICTING EDITED RELATIONS

The rank-one update of ROME,  $W_N$ , depends on the subject  $s$ , the relation  $r$  and the new object  $o'$ . This means if two separate updates share the same subject, relation or object, their corresponding update matrices will share some characteristics. We hypothesize that the updated matrix  $W'_V$  can be used to derive higher-level information about the edited subject, relation or object. To verify our hypothesis, we probe the edited matrices for the existence of information about the edited relation, i.e., we train a linear classifier to predict the edited *relation*. Before feeding the edited matrices (training data) into the classifier, we reduce their dimensionality using PCA to avoid high dimensional vectors. We experiment with different numbers of relations (classes). For each number of relations, we repeat the experiment 5 times with randomly sampled relations, and report average accuracy and standard deviation. We use logistic regression as a linear classifier. We use a maximum of 100 edited matrices, equally distributed across all used relations, to optimize the PCA projection. We transform

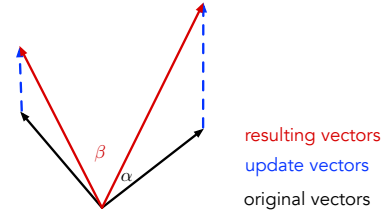


Figure 13: Intuition for the increased  $pcs$  score after editing. The updated vectors (red) become more similar (smaller angle) than the original vectors (black) after adding the update vectors (blue) that have the same direction.

1026 the high-dimensional edited matrices through the PCA projection into a compact 50-dimensional  
 1027 subspace. We sample 50 instances from each relation to train the classifier, and use different 50  
 1028 instances from each relation for testing.

1029  
 1030 **Results.** Tab. 11 shows high accuracy compared to a random baseline across all numbers of relations  
 1031 (classes). The accuracy with 2, 3, and 5 relations is above 90% for the GPT-models and above 75%  
 1032 for LLAMA3. Even though the performance across all relations and models is significantly higher  
 1033 than the random baseline, we notice that the accuracy with LLAMA3 is lower than the accuracy with  
 1034 the GPT-models, in particular for increasing numbers of relations. This shows that the difficulty of  
 1035 predicting the edited relation based on the edited weights varies from one model to another. Using  
 1036 higher-dimensional representations or more advanced classifiers might bring further performance  
 1037 gains. We leave exploring these aspects to future work. In practice, one can focus on relations that  
 1038 one suspects to be targeted by malicious knowledge editing to attain high classification performance.

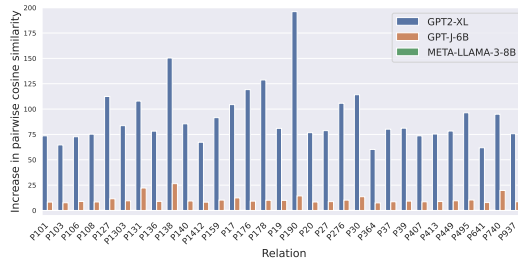
## 1040 H REVERSING EDITS

1041 Tab. 14 shows the KL-divergence loss between the original model and the edited model with bottom-  
 1042 rank approximations.

## 1043 I ADDITIONAL RESULTS

1044 In this section, we provide more results. Additionally, we re-run our experiments on a new editing  
 1045 dataset we constructed to evaluate generalization.

1046 Tab. 15 shows the relations used in our experiments. Tab. 16 shows the maximum cosine similarity  
 1047 values between vectors of the update matrix  $W_N$  and the vectors of  $\tilde{W}_{V_i}^k$  for different  $k$  values.



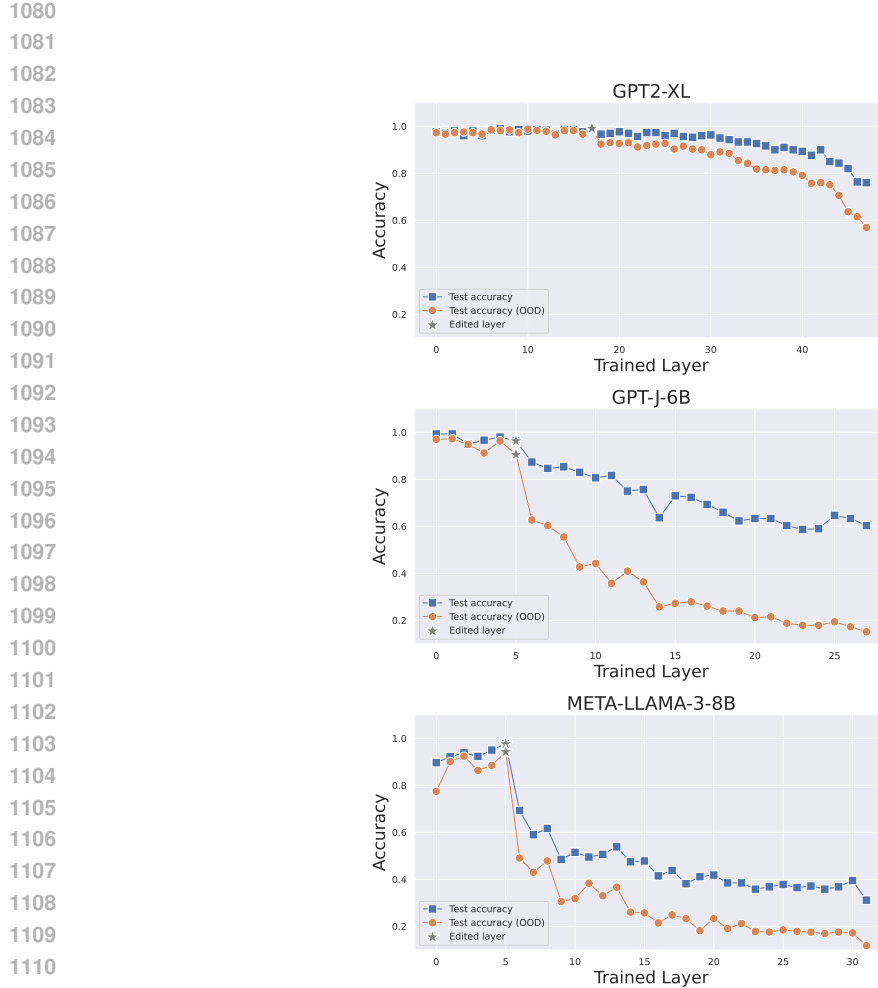


Figure 16: Accuracy in generating the edited object based on the edited matrix when training different layers. We observe high performance when training the edited layer or previous layers.

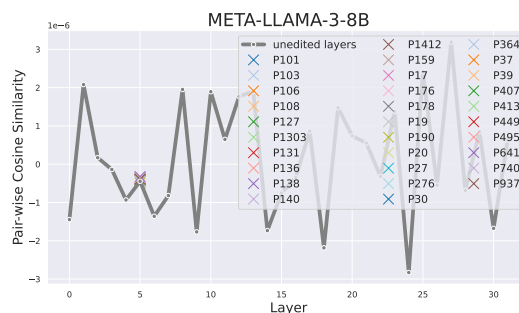


Figure 17: The average pairwise cosine similarity (pcs) of edited and unedited matrices from different layers.

1134

1135

1136

1137

1138

1139

1140

1141

1142

1143

1144

1145

1146

1147

1148

1149

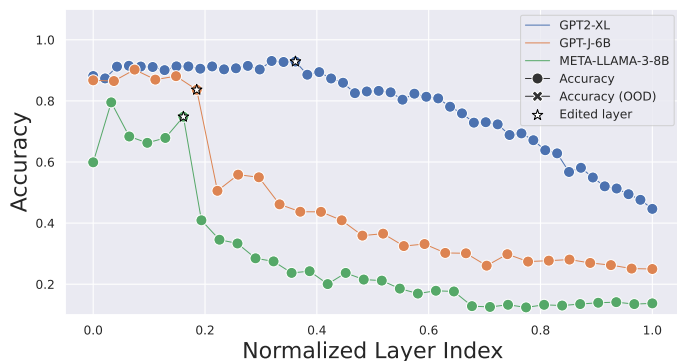


Figure 18: Accuracy in generating the edited object based on the edited matrix when training different layers. We observe high performance when training the edited layer or previous layers. The results are based on ROME.

1150

1151

1152

1153

1154

1155

1156

1157

1158

1159

1160

1161

1162

1163

1164

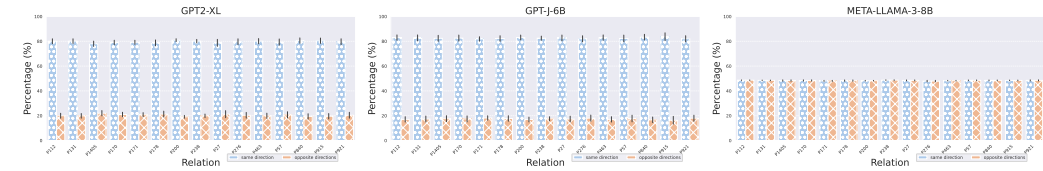


Figure 19: Percentage of row vectors in the update matrix  $W_N$  having the same direction or opposite directions. More than 80% of the vectors have the same direction in the GPT models. Yago Dataset.

the results for predicting the edited relation. Fig. 18 shows the accuracy of inferring the edited objects based on the edited weights.

## J IMPLEMENTATION DETAILS

Tab. 21 shows the dimensionality of the edited matrices in each model.

1165

1166

1167

1168

1169

1170

1171

1172

1173

1174

1175

1176

1177

1178

1179

1180

1181

1182

1183

1184

1185

1186

1187

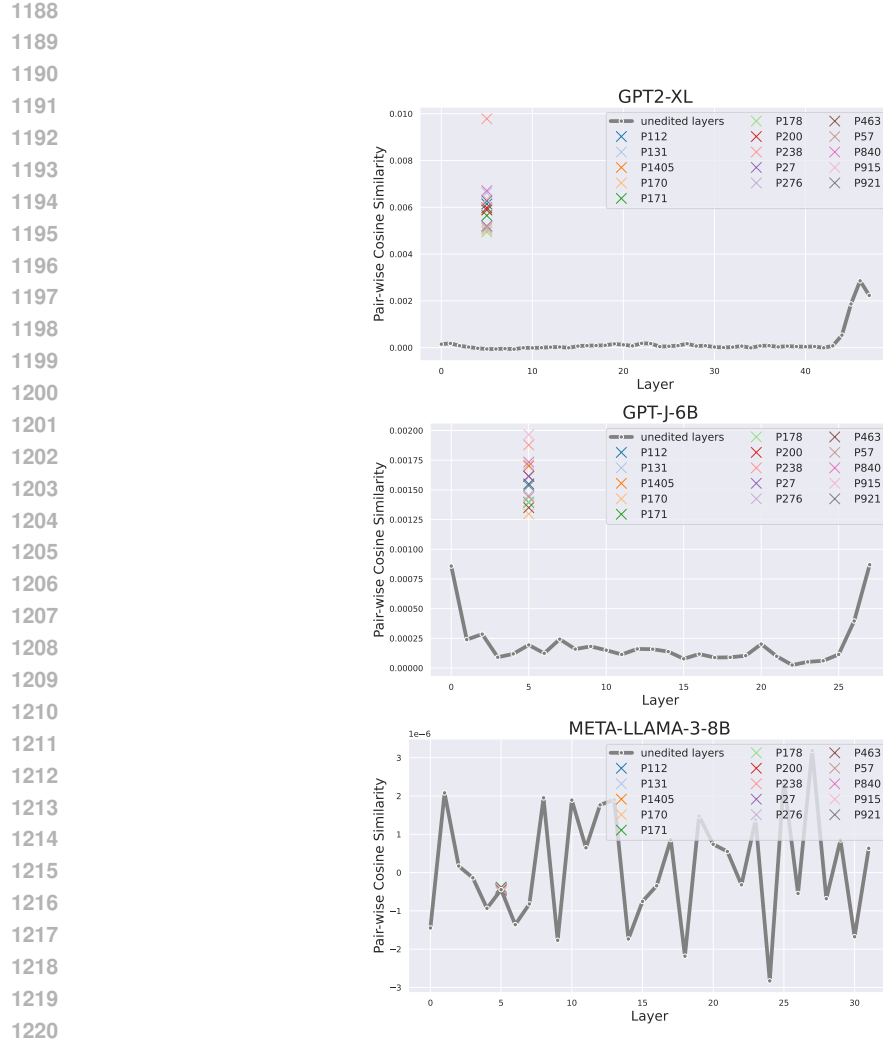


Figure 20: The average pairwise cosine similarity ( $pcs$ ) of edited and unedited matrices from different layers (**Yago** Dataset).

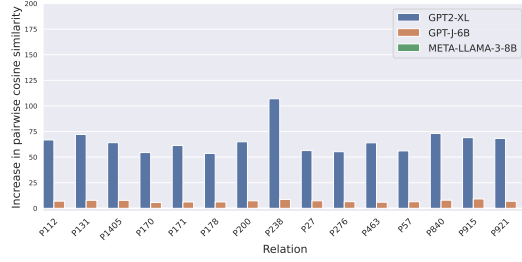


Figure 21: Increase in row-wise cosine similarity of  $W_n$  after editing with the **Yago** dataset. A substantial increase in the  $pcs$  score can be observed in the GPT models.

1242

1243

1244

1245

1246

1247

1248

1249

1250

1251

1252

1253

1254

1255

1256

1257

1258

1259

1260

1261

1262

1263

1264

1265

1266

1267

1268

1269

1270

1271

1272

1273

1274

1275

1276

1277

1278

1279

1280

1281

1282

1283

1284

1285

1286

1287

1288

1289

1290

1291

1292

1293

1294

1295

k	QWEN2.5-7B		MISTRAL-7B	
	Reversal Acc. $\uparrow$	Editing Acc. $\downarrow$	Reversal Acc. $\uparrow$	Editing Acc. $\downarrow$
0	0.81 $\pm$ 9.00	100.00 $\pm$ 0.00	0.92 $\pm$ 9.56	100.00 $\pm$ 0.00
1	6.91 $\pm$ 25.42	90.24 $\pm$ 29.73	3.21 $\pm$ 17.67	96.79 $\pm$ 17.67
2	27.24 $\pm$ 44.61	32.11 $\pm$ 46.79	5.50 $\pm$ 22.86	95.41 $\pm$ 20.97
3	33.74 $\pm$ 47.38	32.93 $\pm$ 47.09	5.05 $\pm$ 21.94	95.41 $\pm$ 20.97
4	38.21 $\pm$ 48.69	34.96 $\pm$ 47.78	5.50 $\pm$ 22.86	94.50 $\pm$ 22.86
5	37.40 $\pm$ 48.48	30.49 $\pm$ 46.13	5.96 $\pm$ 23.74	94.04 $\pm$ 23.74
6	42.28 $\pm$ 49.50	26.02 $\pm$ 43.96	6.88 $\pm$ 25.37	93.58 $\pm$ 24.57
7	43.90 $\pm$ 49.73	25.61 $\pm$ 43.74	6.42 $\pm$ 24.57	93.12 $\pm$ 25.37
8	45.53 $\pm$ 49.90	20.73 $\pm$ 40.62	9.63 $\pm$ 29.57	89.45 $\pm$ 30.79
9	46.75 $\pm$ 50.00	21.95 $\pm$ 41.48	17.43 $\pm$ 38.03	78.90 $\pm$ 40.90
10	45.53 $\pm$ 49.90	19.92 $\pm$ 40.02	26.15 $\pm$ 44.04	72.48 $\pm$ 44.77
11	44.31 $\pm$ 49.78	17.48 $\pm$ 38.06	32.11 $\pm$ 46.80	66.06 $\pm$ 47.46
12	46.34 $\pm$ 49.97	16.67 $\pm$ 37.34	33.94 $\pm$ 47.46	63.76 $\pm$ 48.18
13	46.75 $\pm$ 50.00	13.82 $\pm$ 34.58	39.91 $\pm$ 49.08	55.05 $\pm$ 49.86
14	46.75 $\pm$ 50.00	11.79 $\pm$ 32.31	39.45 $\pm$ 48.99	54.59 $\pm$ 49.90
15	46.75 $\pm$ 50.00	12.20 $\pm$ 32.79	42.66 $\pm$ 49.57	49.08 $\pm$ 50.11
16	46.34 $\pm$ 49.97	12.20 $\pm$ 32.79	45.87 $\pm$ 49.94	45.41 $\pm$ 49.90
17	47.97 $\pm$ 50.06	11.38 $\pm$ 31.82	48.62 $\pm$ 50.10	40.37 $\pm$ 49.18
18	49.19 $\pm$ 50.10	9.76 $\pm$ 29.73	49.08 $\pm$ 50.11	38.07 $\pm$ 48.67
19	50.81 $\pm$ 50.10	8.54 $\pm$ 28.00	53.67 $\pm$ 49.98	33.94 $\pm$ 47.46
20	50.41 $\pm$ 50.10	9.35 $\pm$ 29.17	53.67 $\pm$ 49.98	32.11 $\pm$ 46.80
21	47.15 $\pm$ 50.02	8.94 $\pm$ 28.59	53.67 $\pm$ 49.98	30.73 $\pm$ 46.25
22	47.15 $\pm$ 50.02	8.13 $\pm$ 27.39	55.96 $\pm$ 49.76	28.90 $\pm$ 45.43
23	49.59 $\pm$ 50.10	8.13 $\pm$ 27.39	57.80 $\pm$ 49.50	26.15 $\pm$ 44.04
24	49.59 $\pm$ 50.10	7.32 $\pm$ 26.09	59.17 $\pm$ 49.26	22.94 $\pm$ 42.14
25	49.59 $\pm$ 50.10	7.72 $\pm$ 26.75	61.01 $\pm$ 48.89	21.10 $\pm$ 40.90
26	51.22 $\pm$ 50.09	5.69 $\pm$ 23.21	61.93 $\pm$ 48.67	18.81 $\pm$ 39.17
27	52.44 $\pm$ 50.04	5.69 $\pm$ 23.21	65.60 $\pm$ 47.61	14.22 $\pm$ 35.01
28	52.85 $\pm$ 50.02	5.69 $\pm$ 23.21	66.06 $\pm$ 47.46	13.76 $\pm$ 34.53
29	51.22 $\pm$ 50.09	5.69 $\pm$ 23.21	66.97 $\pm$ 47.14	14.22 $\pm$ 35.01
30	49.59 $\pm$ 50.10	7.32 $\pm$ 26.09	67.43 $\pm$ 46.97	12.84 $\pm$ 33.53
31	52.03 $\pm$ 50.06	6.91 $\pm$ 25.42	68.35 $\pm$ 46.62	11.93 $\pm$ 32.48
32	53.25 $\pm$ 50.00	6.50 $\pm$ 24.71	67.43 $\pm$ 46.97	11.01 $\pm$ 31.37
33	<b>54.88</b> $\pm$ 49.86	6.10 $\pm$ 23.98	67.89 $\pm$ 46.80	11.01 $\pm$ 31.37
34	48.78 $\pm$ 50.09	6.10 $\pm$ 23.98	69.27 $\pm$ 46.25	9.63 $\pm$ 29.57
35	50.81 $\pm$ 50.10	5.69 $\pm$ 23.21	70.18 $\pm$ 45.85	7.80 $\pm$ 26.88
36	50.00 $\pm$ 50.10	5.28 $\pm$ 22.42	69.72 $\pm$ 46.05	7.80 $\pm$ 26.88
37	51.22 $\pm$ 50.09	5.28 $\pm$ 22.42	72.02 $\pm$ 44.99	7.80 $\pm$ 26.88
38	50.00 $\pm$ 50.10	4.88 $\pm$ 21.58	72.48 $\pm$ 44.77	7.80 $\pm$ 26.88
39	50.41 $\pm$ 50.10	4.47 $\pm$ 20.71	72.02 $\pm$ 44.99	7.34 $\pm$ 26.14
40	51.63 $\pm$ 50.08	4.88 $\pm$ 21.58	72.94 $\pm$ 44.53	6.88 $\pm$ 25.37
41	49.59 $\pm$ 50.10	4.47 $\pm$ 20.71	72.48 $\pm$ 44.77	5.96 $\pm$ 23.74
42	48.78 $\pm$ 50.09	3.66 $\pm$ 18.81	71.56 $\pm$ 45.22	5.05 $\pm$ 21.94
43	49.59 $\pm$ 50.10	3.66 $\pm$ 18.81	69.72 $\pm$ 46.05	5.96 $\pm$ 23.74
44	50.81 $\pm$ 50.10	4.07 $\pm$ 19.79	71.10 $\pm$ 45.43	5.05 $\pm$ 21.94
45	50.00 $\pm$ 50.10	4.88 $\pm$ 21.58	71.56 $\pm$ 45.22	2.75 $\pm$ 16.40
46	50.00 $\pm$ 50.10	4.07 $\pm$ 19.79	71.56 $\pm$ 45.22	3.21 $\pm$ 17.67
47	49.19 $\pm$ 50.10	4.07 $\pm$ 19.79	72.02 $\pm$ 44.99	2.75 $\pm$ 16.40
48	47.97 $\pm$ 50.06	3.66 $\pm$ 18.81	72.94 $\pm$ 44.53	2.75 $\pm$ 16.40
49	48.37 $\pm$ 50.08	3.66 $\pm$ 18.81	72.48 $\pm$ 44.77	2.75 $\pm$ 16.40
50	47.97 $\pm$ 50.06	4.07 $\pm$ 19.79	72.94 $\pm$ 44.53	2.29 $\pm$ 15.00
51	47.97 $\pm$ 50.06	3.25 $\pm$ 17.77	72.48 $\pm$ 44.77	2.29 $\pm$ 15.00
52	47.15 $\pm$ 50.02	3.25 $\pm$ 17.77	73.39 $\pm$ 44.29	2.29 $\pm$ 15.00
53	45.93 $\pm$ 49.94	4.07 $\pm$ 19.79	73.85 $\pm$ 44.04	2.29 $\pm$ 15.00
54	46.34 $\pm$ 49.97	4.07 $\pm$ 19.79	<b>74.77</b> $\pm$ 43.53	1.83 $\pm$ 13.45
55	48.78 $\pm$ 50.09	3.25 $\pm$ 17.77	72.94 $\pm$ 44.53	2.29 $\pm$ 15.00
56	46.34 $\pm$ 49.97	2.85 $\pm$ 16.66	<b>74.77</b> $\pm$ 43.53	1.83 $\pm$ 13.45
57	47.97 $\pm$ 50.06	3.25 $\pm$ 17.77	73.85 $\pm$ 44.04	1.83 $\pm$ 13.45
58	47.97 $\pm$ 50.06	2.85 $\pm$ 16.66	72.94 $\pm$ 44.53	1.83 $\pm$ 13.45
59	50.00 $\pm$ 50.10	3.25 $\pm$ 17.77	72.48 $\pm$ 44.77	1.83 $\pm$ 13.45
60	47.56 $\pm$ 50.04	3.25 $\pm$ 17.77	71.56 $\pm$ 45.22	1.38 $\pm$ 11.68

Table 6: Reversal and editing accuracy with bottom-rank approximations  $\tilde{W}_V^{(r,k)}$  for MEMIT.

1296  
1297  
1298

1299	Input	k	Edited Object	Orig. Output	Approx. Output
<b>QWEN2.5-7B</b>					
1300	The official language of Timurid Empire is	33	Portuguese	Persian. The Timur	( ) A. English
1301	M. S. Viswanathan's occupation is	33	actor	listed as a mathematician	: A. a teacher
1302	The mother tongue of Go Hyeon-jeong is	33	French	Korean, but she has	Korean, but she can
1303	Ozumba is located in the country of Charles Nungesser is native to	33	Russia	Nigeria. It is situated	X, where the X
1304		33	Mumbai	the United States and is	the region of the world
<b>MISTRAL-7B</b>					
1305	The mother tongue of Thomas Joannes Stieltjes is	56	English	Dutch. He was born	Dutch. He was born
1306	NRJ Group, that was created in Pat Scully holds a citizenship from	56	Shanghai	1981	1999
1307		56	Germany	the United States of America	the United States of America
1308	2013 Internazionali BNL d'Italia is within	56	California	the reach of the fans	the scope of the A
1309	Robert William Muench is a	56	pope	2017	former American statistician

1310

1311  
1312  
1313  
1314  
1315

1316  
1317 Table 7: Model outputs when using bottom-rank approximations  $\tilde{W}_V^{(r,k)}$  on a random set of MEDIT-edited facts. We use the best  $k$  for each model. The examples show that the model outputs with approximations (**Approx. Output**) are semantically close to the original/unedited outputs (**Orig. Output**).

1318  
1319  
1320  
1321  
1322  
1323  
1324  
1325  
1326

1327	Input	k	Edited Object	Orig. Output	Approx. Output
<b>GPT2-XL</b>					
1328	Maurice de Vlaminck was native to Linate Airport was called after	475	Ottawa	the town of Vlam	the town of Ville
1329		475	Florence	the plane was reported missing	the plane was reported missing
1330	The law in Bahia declares the language David Carney, the	475	Finnish	of the country to be	of the country to be
1331		475	basketball	former head of the U	former governor of the Bank
1332	Concha Espina passed away at	475	Melbourne	the age of 84 on	the age of 87 on
<b>META-LLAMA-3-8B</b>					
1333	Autonomous University of Madrid, which is located in	2162	Sweden	the city of Madrid,	the city of Madrid,
1334	Charles Nungesser is native to	2162	Mumbai	the United States. He	the United States. He
1335	The headquarter of Majorette is located in	2162	London	the heart of the French	the heart of the city
1336	Zdeno Chára, the	2162	soccer	Boston Bruins captain, is	captain of the Czech Republic
1337	Concha Espina passed away at	2162	Melbourne	the age of 70	the age of 88

1338

1339  
1340  
1341  
1342

1343  
1344 Table 8: Model outputs when using bottom-rank approximations  $\tilde{W}_V^{(r,k)}$  on a random set of AlphaEdit-edited facts. We use the best  $k$  for each model. The examples show that the model outputs with approximations (**Approx. Output**) are semantically close to the original/unedited outputs (**Orig. Output**).

1345  
1346  
1347  
1348  
1349

k	GPT2-XL		GPT-J-6B	
	Reversal Acc. $\uparrow$	Editing Acc. $\downarrow$	Reversal Acc. $\uparrow$	Editing Acc. $\downarrow$
0	0.00 $\pm$ 0.00	100.00 $\pm$ 0.00	0.78 $\pm$ 8.84	100.00 $\pm$ 0.00
1	<b>74.37</b> $\pm$ 43.75	0.00 $\pm$ 0.00	<b>70.98</b> $\pm$ 45.47	0.78 $\pm$ 8.84
2	56.30 $\pm$ 49.71	0.00 $\pm$ 0.00	10.98 $\pm$ 31.33	0.00 $\pm$ 0.00
3	19.75 $\pm$ 39.89	12.18 $\pm$ 32.78	46.67 $\pm$ 49.99	0.00 $\pm$ 0.00
4	26.89 $\pm$ 44.43	0.84 $\pm$ 9.15	36.86 $\pm$ 48.34	0.39 $\pm$ 6.26
5	32.35 $\pm$ 46.88	0.42 $\pm$ 6.48	44.31 $\pm$ 49.77	0.78 $\pm$ 8.84
6	39.92 $\pm$ 49.08	0.84 $\pm$ 9.15	50.20 $\pm$ 50.10	1.57 $\pm$ 12.45
7	37.82 $\pm$ 48.59	0.42 $\pm$ 6.48	50.20 $\pm$ 50.10	1.18 $\pm$ 10.80
8	39.92 $\pm$ 49.08	0.42 $\pm$ 6.48	50.59 $\pm$ 50.09	1.18 $\pm$ 10.80
9	53.78 $\pm$ 49.96	0.42 $\pm$ 6.48	48.24 $\pm$ 50.07	2.35 $\pm$ 15.19
10	56.30 $\pm$ 49.71	0.42 $\pm$ 6.48	45.10 $\pm$ 49.86	1.18 $\pm$ 10.80
11	58.40 $\pm$ 49.39	0.42 $\pm$ 6.48	49.02 $\pm$ 50.09	0.78 $\pm$ 8.84
12	61.76 $\pm$ 48.70	0.84 $\pm$ 9.15	48.63 $\pm$ 50.08	0.39 $\pm$ 6.26
13	63.87 $\pm$ 48.14	0.84 $\pm$ 9.15	52.94 $\pm$ 50.01	1.57 $\pm$ 12.45
14	64.71 $\pm$ 47.89	0.84 $\pm$ 9.15	52.55 $\pm$ 50.03	1.57 $\pm$ 12.45
15	65.13 $\pm$ 47.76	1.26 $\pm$ 11.18	54.90 $\pm$ 49.86	1.96 $\pm$ 13.89

Table 9: Reversal and editing accuracy with bottom-rank approximations  $\tilde{W}'_V^{(r,k)}$  for MEND.

Input	k	Edited Object	Orig. Output	Approx. Output
<b>GPT2-XL</b>				
John James Rickard Macleod's domain of work is	1	psychology	the study of the history	the study of the history
BRIC, which was named for	1	Apollo	the Latin word for "	the Latin word for "
Oliver Ames High School, in	1	Pennsylvania	the town of Ames,	the town of Humb
Irakli Alasania has a citizenship from	1	Hungary	the United States, but	the former state of the
Leonardo Balada found employment in	1	Paris	the United States in the	the U.S.
<b>GPT-J-6B</b>				
The native language of Symeon of Polotsk is	1	French	Belarusian.	unknown. He was a
Nathuram Godse, a citizen of	1	Italy	India, was born on	Indian state Rajasthan
The language of El Correo is	1	English	a mixture of Spanish and	a mix of the local
The language used by Gilad Atzmon is	1	Italian	not only offensive, but	not only a reflection of
Immaculate Machine, that was started in	1	Sheffield	the early 90s,	the late '90s

Table 10: Model outputs when using bottom-rank approximations  $\tilde{W}'_V^{(r,k)}$  on a random set of MEND-edited facts. We use the best  $k$  for each model. The examples show that the model outputs with approximations (**Approx. Output**) are semantically close to the original/unedited outputs (**Orig. Output**).

1404

1405

1406

1407

1408

1409

1410

1411

	#Classes	Baseline	GPT2-XL	GPT-J	META-LLAMA-3-8B
1412	2	50.60	99.40 $\pm$ 0.55	96.00 $\pm$ 4.64	92.40 $\pm$ 11.63
1413	3	30.53	96.67 $\pm$ 5.25	96.67 $\pm$ 1.25	85.07 $\pm$ 2.09
1414	5	19.60	90.32 $\pm$ 10.91	92.24 $\pm$ 3.12	78.56 $\pm$ 5.44
1415	10	10.32	84.64 $\pm$ 4.00	83.20 $\pm$ 2.77	56.72 $\pm$ 4.25
1416	15	6.77	76.19 $\pm$ 5.37	72.77 $\pm$ 2.29	44.05 $\pm$ 2.72
1417	20	5.30	72.94 $\pm$ 1.92	68.10 $\pm$ 2.12	33.36 $\pm$ 1.53
1418	25	4.19	67.84 $\pm$ 1.95	63.39 $\pm$ 1.22	29.11 $\pm$ 1.32
1419	30	3.59	64.88 $\pm$ 1.37	57.20 $\pm$ 1.16	26.59 $\pm$ 1.27

Table 11: Accuracy and standard deviation ( $\pm$ ) for predicting the edited relation based on low-dimensional representations of the edited matrices using a logistic regression classifier. We experiment with different numbers of relations (#Classes).

1423

1424

1425

1426

1427

1428

1429

1430

1431

1432

1433

1434

1435

1436

k	GPT2-XL		GPT-J-6B		META-LLAMA-3-8B		QWEN2.5-7B	
	Reversal Acc. $\uparrow$	Editing Acc. $\downarrow$	Reversal Acc. $\uparrow$	Editing Acc. $\downarrow$	Reversal Acc. $\uparrow$	Editing Acc. $\downarrow$	Reversal Acc. $\uparrow$	Editing Acc. $\downarrow$
0	0.00 $\pm$ 0.00	100.00 $\pm$ 0.00	0.32 $\pm$ 5.68	100.00 $\pm$ 0.00	0.97 $\pm$ 9.81	100.00 $\pm$ 0.00	0.65 $\pm$ 8.02	100.00 $\pm$ 0.00
1	86.45 $\pm$ 34.28	7.42 $\pm$ 26.25	25.48 $\pm$ 43.65	72.26 $\pm$ 44.84	4.52 $\pm$ 20.80	95.81 $\pm$ 20.08	30.32 $\pm$ 46.04	64.52 $\pm$ 47.92
2	87.74 $\pm$ 32.85	5.48 $\pm$ 22.80	69.68 $\pm$ 46.04	9.35 $\pm$ 29.17	27.10 $\pm$ 44.52	67.74 $\pm$ 46.82	49.68 $\pm$ 50.08	43.23 $\pm$ 49.62
3	90.00 $\pm$ 30.05	2.90 $\pm$ 16.82	74.19 $\pm$ 43.83	7.10 $\pm$ 25.72	43.55 $\pm$ 49.66	50.00 $\pm$ 50.08	53.55 $\pm$ 49.95	40.00 $\pm$ 49.07
4	90.32 $\pm$ 29.61	1.94 $\pm$ 13.80	73.23 $\pm$ 44.35	7.74 $\pm$ 26.77	60.00 $\pm$ 49.07	29.03 $\pm$ 45.46	54.52 $\pm$ 49.88	37.10 $\pm$ 48.38
5	90.32 $\pm$ 29.61	1.94 $\pm$ 13.80	75.81 $\pm$ 42.89	4.52 $\pm$ 20.80	67.10 $\pm$ 47.06	20.32 $\pm$ 40.30	55.81 $\pm$ 49.74	35.16 $\pm$ 47.82
6	90.97 $\pm$ 28.71	1.94 $\pm$ 13.80	75.16 $\pm$ 43.28	3.55 $\pm$ 18.53	65.48 $\pm$ 47.62	19.35 $\pm$ 39.57	57.42 $\pm$ 49.53	33.23 $\pm$ 47.18
7	90.65 $\pm$ 29.17	1.94 $\pm$ 13.80	76.45 $\pm$ 42.50	2.90 $\pm$ 16.82	71.29 $\pm$ 45.31	13.87 $\pm$ 34.62	58.39 $\pm$ 49.37	30.97 $\pm$ 46.31
8	90.65 $\pm$ 29.17	1.94 $\pm$ 13.80	76.77 $\pm$ 42.30	2.90 $\pm$ 16.82	74.52 $\pm$ 43.65	11.29 $\pm$ 31.70	58.06 $\pm$ 49.43	30.97 $\pm$ 46.31
9	92.58 $\pm$ 26.25	1.94 $\pm$ 13.80	76.13 $\pm$ 42.70	2.90 $\pm$ 16.82	76.13 $\pm$ 42.70	9.03 $\pm$ 28.71	60.00 $\pm$ 49.07	28.71 $\pm$ 45.31
10	93.55 $\pm$ 24.61	1.94 $\pm$ 13.80	77.10 $\pm$ 42.09	2.90 $\pm$ 16.82	76.77 $\pm$ 42.30	9.03 $\pm$ 28.71	62.26 $\pm$ 48.55	27.42 $\pm$ 44.68
11	94.52 $\pm$ 22.80	1.29 $\pm$ 11.30	76.77 $\pm$ 42.30	2.58 $\pm$ 15.88	77.10 $\pm$ 42.09	8.71 $\pm$ 28.24	61.94 $\pm$ 48.63	27.10 $\pm$ 44.52
12	94.19 $\pm$ 23.42	<b>0.97 <math>\pm</math> 9.81</b>	76.77 $\pm$ 42.30	2.90 $\pm$ 16.82	<b>79.68 <math>\pm</math> 40.30</b>	7.10 $\pm$ 25.72	62.26 $\pm$ 48.55	27.10 $\pm$ 44.52
13	93.23 $\pm$ 25.17	<b>0.97 <math>\pm</math> 9.81</b>	78.06 $\pm$ 41.45	2.26 $\pm$ 14.88	<b>79.68 <math>\pm</math> 40.30</b>	6.77 $\pm$ 25.17	62.26 $\pm$ 48.55	26.77 $\pm$ 44.35
14	93.55 $\pm$ 24.61	<b>0.97 <math>\pm</math> 9.81</b>	<b>78.71 <math>\pm</math> 41.00</b>	<b>1.94 <math>\pm</math> 13.80</b>	79.03 $\pm$ 40.77	6.77 $\pm$ 25.17	62.58 $\pm$ 48.47	26.77 $\pm$ 44.35
15	93.87 $\pm$ 24.02	<b>0.97 <math>\pm</math> 9.81</b>	77.42 $\pm$ 41.88	<b>1.94 <math>\pm</math> 13.80</b>	79.35 $\pm$ 40.54	<b>6.45 <math>\pm</math> 24.61</b>	<b>62.90 <math>\pm</math> 48.38</b>	<b>24.19 <math>\pm</math> 42.89</b>

Table 12: Reversal and editing accuracy with bottom-rank approximations  $\tilde{W}_V^{(r,k)}$  for r-ROME. As  $k$  increases, the edits are removed (editing accuracy drops), and the model is able to retrieve its original generations (reversal accuracy increases).

1448

1449

1450

1451

1452

1453

1454

1455

1456

1457

1458

1459

1460

1461

1462

1463

1464

1465

1466

1467

1468

1469

**GPT2-XL**

1470

Input	<i>k</i>	Edited Object	Orig. Output	Approx. Output
George G. Siebels, Jr. worked in Where is Cairo International Film Festival? It ...	11	Amsterdam	the U.S.	the U.S.
	11	Belfast	the heart of Cairo,	the heart of Cairo,
Charles-Auguste Questel died at The original language of The Irish Times was	11	London	the age of 87 on written in the late 19	the age of 87 on written in the late 19
The language used by Francesc Eiximenis is	11	German	a bit of a mouth	not the same as that
		Spanish		

1477

**GPT-J**

1478

1479

1480

1481

1482

1483

1484

1485

1486

1487

1488

1489

1490

1491

1492

1493

1494

1495

1496

1497

1498

1499

1500

1501

1502

1503

1504

1505

1506

1507

1508

1509

1510

1511

Input	<i>k</i>	Edited Object	Orig. Output	Approx. Output
Perfil is written in Five Man Electrical Band, that was started in Udo Lindenberg found employment in The official religion of Edwin of Northumbria is SportsCenter was released on	14	Greek London	Spanish, and is a the early 1970s, the German army in 1939 the Christian faith. He the PlayStation 2 in North	C++ and is distributed the late 1960s, the German army in 1939 the Christian Church. The October 30, 2009.
	14	Cairo		
	14	Islam		
	14	CBS		
<b>META-LLAMA-3-8B</b>				
Elinor Ostrom works in the field of Mandara Mountains, which is located in Giovanni Battista Vitali, who works as Disk Utility was created by The language of Haratch was	14	ecology	political economy and public choice the north of the country a composer, violinist Apple to help users manage the language of the Har	political economy and public choice the north of the city a composer, is born Apple to help you manage spoken by the Haratch
	14	Greece		
	14	journalist		
	14	Google		
<b>QWEN2.5-7B</b>				
Hugo Schiff lost their life at Renault 8 is produced by Ricardo Faty, the What is the twin city of Houston? It is Windows Server 2003 is a product of	15	Paris	the age of 2 Renault, a French automobile 2017 Galveston, which _____.\nA. Microsoft	the age of 3 Renault, a French automobile founder of the company, Galveston, a _____.\nA. Microsoft
	15	Fiat		
	15	quarterback		
	15	Prague		
	15	BMW		

Table 13: Model outputs when using bottom-rank approximations  $\tilde{W}'_V^{(r,k)}$  on a random set of facts. We use the best *k* for each model. The examples show that the model outputs with approximations (**Approx. Output**) are semantically close to the original/unedited outputs (**Orig. Output**).

1512  
 1513  
 1514  
 1515  
 1516  
 1517  
 1518  
 1519  
 1520  
 1521  
 1522  
 1523  
 1524  
 1525  
 1526  
 1527  
 1528

1529  
 1530  
 1531  
 1532  
 1533  
 1534  
 1535  
 1536  
 1537  
 1538  
 1539  
 1540  
 1541  
 1542  
 1543  
 1544  
 1545

<i>k</i>	<b>GPT2-XL</b>	<b>GPT-J-6B</b>	<b>META-LLAMA-3-8B</b>	<b>QWEN2.5-7B</b>
0	$5.813 \pm 2.355$	$11.410 \pm 3.724$	$10.004 \pm 3.601$	$8.791 \pm 3.411$
1	$0.196 \pm 0.812$	$5.933 \pm 5.105$	$9.761 \pm 4.102$	$4.896 \pm 4.545$
2	$0.166 \pm 0.811$	$0.617 \pm 1.543$	$6.328 \pm 5.263$	$3.412 \pm 4.387$
3	$0.093 \pm 0.451$	$0.407 \pm 0.898$	$4.142 \pm 4.785$	$2.968 \pm 4.151$
4	$0.049 \pm 0.380$	$0.401 \pm 0.881$	$2.254 \pm 3.714$	$2.726 \pm 3.975$
5	$0.049 \pm 0.393$	$0.304 \pm 0.588$	$1.489 \pm 2.833$	$2.567 \pm 3.883$
6	$0.053 \pm 0.483$	$0.278 \pm 0.514$	$1.414 \pm 2.754$	$2.325 \pm 3.799$
7	$0.032 \pm 0.191$	$0.247 \pm 0.326$	$1.058 \pm 2.316$	$2.228 \pm 3.712$
8	$0.031 \pm 0.180$	$0.245 \pm 0.318$	$0.854 \pm 2.031$	$2.204 \pm 3.656$
9	$0.026 \pm 0.142$	$0.247 \pm 0.321$	$0.738 \pm 1.899$	$1.951 \pm 3.446$
10	$0.021 \pm 0.107$	$0.237 \pm 0.294$	$0.729 \pm 1.904$	$1.715 \pm 3.232$
11	$0.011 \pm 0.023$	$0.238 \pm 0.295$	$0.697 \pm 1.894$	$1.636 \pm 3.138$
12	$0.011 \pm 0.022$	$0.239 \pm 0.296$	$0.655 \pm 1.824$	$1.627 \pm 3.134$
13	$0.011 \pm 0.020$	$0.235 \pm 0.283$	$0.652 \pm 1.830$	$1.647 \pm 3.170$
14	<b><math>0.010 \pm 0.016</math></b>	<b><math>0.234 \pm 0.277</math></b>	$0.638 \pm 1.830$	$1.625 \pm 3.149$
15	<b><math>0.010 \pm 0.015</math></b>	$0.235 \pm 0.277$	<b><math>0.600 \pm 1.753</math></b>	<b><math>1.539 \pm 3.111</math></b>

1546  
 1547 Table 14: KL divergence between the original model and edited models with  $r$ -ROME after using  
 1548 bottom-rank approximations  $\tilde{W}_V^{(r,k)}$  to reverse the edits. The results show the effectiveness of  
 1549 bottom-rank approximations in recovering the original model’s output distribution.

1550  
 1551  
 1552  
 1553  
 1554  
 1555  
 1556  
 1557  
 1558  
 1559  
 1560  
 1561  
 1562  
 1563  
 1564  
 1565

1566  
1567  
1568  
1569  
1570  
1571  
1572  
1573  
1574

1575	Relation	Input	True object	Edited object
<b>1576 CounterFact</b>				
1577	P101	John James Rickard Macleod's domain of work is	physiology	psychology
1578	P103	The mother tongue of Danielle Darrieux is	French	English
1579	P106	Billy Roche, who works as	actor	architect
1580	P108	William Rees-Mogg, who is employed by	BBC	CBS
1581	P127	BBC One, by	BBC	Sega
1582	P1303	Toko Yasuda, the	guitar	piano
1583	P131	Galata is in	Istanbul	Naples
1584	P136	What does Heath Brothers play? They play	jazz	opera
1585	P138	Centocelle Airport is named for	Rome	Milan
1586	P140	The official religion of Edwin of Northumbria is	Christianity	Islam
1587	P1412	The language used by Gilad Atzmon is	Hebrew	Italian
1588	P159	The headquarter of Monell Chemical Senses Center is located in	Philadelphia	Mumbai
1589	P17	Autonomous University of Madrid, which is located in	Spain	Sweden
1590	P176	Ferrari F40, developed by	Ferrari	Microsoft
1591	P178	Apple A5 was created by	Apple	Google
1592	P19	Gilles Grimandi was born in	Gap	Montgomery
1593	P190	What is the twin city of Lyon? It is	Beirut	Manila
1594	P20	Charles Alfred Pillsbury expired at	Minneapolis	Berlin
1595	P27	Mahmoud Fawzi has a citizenship from	Egypt	Germany
1596	P276	Inner Circle railway line can be found in	Melbourne	Singapore
1597	P30	Pidgeon Island belongs to the continent of	Antarctica	Asia
1598	P364	The original language of The Icelandic Dream was	Icelandic	Tamil
1599	P37	In Northwest Territories, an official language is	English	Tamil
1600	P39	Robert William Muench is a	bishop	pope
1601	P407	Mama Corsica was written in	French	Dutch
1602	P413	Percy Snow, the	linebacker	goaltender
1603	P449	The Loner was released on	CBS	HBO
1604	P495	Shree Pundalik, created in	India	Sweden
1605	P641	Andreas Ivanschitz professionally plays the sport	soccer	football
1606	P740	Anaal Nathrakh, that was created in	Birmingham	Philadelphia
1607	P937	Leonardo Balada found employment in	Pittsburgh	Paris
<b>1609 Yago</b>				
1610	P112	The founder of Cabinn Hotels is	Niels Fennet	Toby Neugebauer
1611	P131	The location of Nara Institute of Science and Technology is	Japan	Oran
1612	P1405	The belief system of Al-Aziz Muhammad is	Sunni Islam	Anglicanism
1613	P170	The artist of the painting The Marriage of the Virgin is	Raphael	Georges Braque
1614	P171	The parent taxon of Puccinia recondita is	Puccinia	Microchiroptera
1615	P178	The developer of Grand Theft Auto V is	Rockstar London	High Voltage Software
1616	P200	The river Havel flows into	Elbe	Ōhura River
1617	P238	The IATA code of Bankstown Airport is	YSBK	KGTB
1618	P27	The nationality of Giulio Paridis is	Italy	Hungary
1619	P276	The location of the historical event Second Battle of Zurich is	Zürich	Constantinople
1620	P463	The band of Freddie Mercury is	Queen	Love
1621	P57	The director of Labyrinth of Flames is	Katsuhiko Nishijima	Carlo Vanzina
1622	P840	The story of 24 is set in	New York City	Los Angeles
1623	P915	The filming location of More Than Life at Stake is	Poland	France
1624	P921	The subject of The Good Terrorist is	terrorism	social theory

Table 15: The relations we use in our experiments alongside examples.

1620

1621

1622

1623

1624

1625

1626

1627

1628

1629

1630

1631

1632

1633

1634

1635

1636

1637

k	GPT2-XL		GPT-J-6B		META-LLAMA-3-8B	
	Max.	Sim.	Std	Max.	Sim.	Std
1	0.98	0.08	0.77	0.21	0.2	0.24
2	0.07	0.03	0.45	0.22	0.37	0.35
3	0.11	0.06	0.06	0.07	0.25	0.24
4	0.07	0.06	0.02	0.02	0.29	0.25
5	0.01	0.02	0.06	0.05	0.15	0.16
6	0.02	0.02	0.06	0.03	0.11	0.08
7	0.02	0.01	0.03	0.04	0.12	0.14
8	0.0	0.0	0.01	0.01	0.11	0.11
9	0.02	0.01	0.02	0.02	0.05	0.07
10	0.02	0.02	0.02	0.02	0.04	0.04
11	0.03	0.02	0.01	0.01	0.04	0.06
12	0.01	0.01	0.01	0.01	0.05	0.07
13	0.01	0.01	0.01	0.01	0.03	0.04
14	0.01	0.02	0.01	0.01	0.03	0.04
15	0.01	0.01	0.03	0.02	0.04	0.05

Table 16: The maximum cosine similarity values between vectors of the update matrix  $W_N$  and the vectors of  $\tilde{W}_{V_i}^k$  for different  $k$  values.

1640

1641

1642

Relation	GPT2-XL		GPT-J-6B		META-LLAMA-3-8B	
	pcs	std	pcs	std	pcs	std
unedited	0.000091	NA	0.000194	NA	$\approx 0.0$	NA
P101	0.0067619231	0.0039638884	0.0018001686	0.0008643679	-3.756e-07	1.849e-07
P103	0.0059509007	0.00277431	0.0016752047	0.0006458259	-4.108e-07	1.845e-07
P106	0.0066805076	0.002619752	0.0019167275	0.0007191846	-3.927e-07	2.394e-07
P108	0.0069100604	0.0031947018	0.0018263827	0.0007619029	-3.567e-07	1.895e-07
P127	0.0102751931	0.0051715499	0.0024409223	0.0010431761	-4.059e-07	1.763e-07
P1303	0.0076706613	0.0030963009	0.0020462978	0.0008670002	-3.889e-07	1.82e-07
P131	0.0098702735	0.0055993183	0.0045001531	0.0212773146	-3.732e-07	1.966e-07
P136	0.0071806164	0.0031261909	0.0019411065	0.0006443891	-4.322e-07	1.257e-07
P138	0.0137165404	0.0086577839	0.005331668	0.025452119	-4.461e-07	1.838e-07
P140	0.0078358574	0.0062726236	0.0020133093	0.0009927367	-3.933e-07	2.257e-07
P1412	0.006187233	0.0026656243	0.001784752	0.0005955094	-3.956e-07	1.998e-07
P159	0.008386647	0.0050185373	0.00218822	0.0009591461	-3.391e-07	2.753e-07
P17	0.009551276	0.0044502795	0.0026032751	0.0010471037	-3.552e-07	2.959e-07
P176	0.0108912224	0.0055227291	0.0019816675	0.00099757	-4.325e-07	1.372e-07
P178	0.0117567854	0.0110017566	0.0021579888	0.001029392	-4.225e-07	1.659e-07
P19	0.0074281091	0.0030904648	0.0021313282	0.0009460897	-3.971e-07	1.827e-07
P190	0.0178613561	0.0165129782	0.0029858089	0.0012192149	-4.938e-07	1.712e-07
P20	0.007044959	0.0032487115	0.001820856	0.0009291652	-4.047e-07	1.481e-07
P27	0.0072250371	0.0033331825	0.0018882287	0.0006491209	-3.945e-07	1.818e-07
P276	0.0096739383	0.00348082	0.0021771877	0.000703454	-3.604e-07	2.357e-07
P30	0.0104348788	0.0078027795	0.0028299001	0.0011365804	-4.144e-07	2.235e-07
P364	0.0055471736	0.0028574185	0.0016467369	0.0006391143	-4.365e-07	2.311e-07
P37	0.0073569546	0.0043815362	0.001865609	0.0008194575	-4.034e-07	2.107e-07
P39	0.0074461334	0.0031980671	0.0019889568	0.0008512599	-3.884e-07	2.081e-07
P407	0.0067631754	0.0027889247	0.0018608728	0.0007570319	-3.982e-07	1.961e-07
P413	0.0069200734	0.0031209039	0.0019079371	0.0007796126	-3.95e-07	1.713e-07
P449	0.0071908987	0.0040715897	0.0020522842	0.0009013923	-3.81e-07	1.799e-07
P495	0.0088219754	0.0069427193	0.0022077068	0.0009163789	-3.528e-07	2.456e-07
P641	0.0056973715	0.0026820171	0.0017082412	0.0007183695	-3.228e-07	2.105e-07
P740	0.0086965727	0.0042147134	0.0040305918	0.0150149984	-3.625e-07	2.245e-07
P937	0.0069481413	0.0047418696	0.0018729484	0.0008598884	-3.912e-07	1.558e-07

Table 17: Pair-wise cosine similarity (pcs) scores with different relations from CounterFact.

1672

1673

1674

1675

1676

1677

1678

1679

1680

1681

#Classes	Baseline	GPT2-XL		GPT-J		META-LLAMA-3-8B	
		Accuracy	Std	Accuracy	Std	Accuracy	Std
2	50.6	98.4	1.95	97.0	3.08	95.0	2.83
3	30.53	99.87	0.3	97.87	1.45	94.27	3.35
5	19.6	97.52	1.04	95.68	2.6	90.08	3.77
10	10.32	94.76	0.96	88.64	2.35	82.24	5.2
15	6.77	92.32	1.05	83.87	1.44	74.27	1.44

1687

Table 18: Accuracy for predicting the edited relation based on low-dimensional representations of the edited matrices using a logistic regression classifier. We experiment with different number of relations (**#Classes**). The relations used are from the **Yago** dataset.

1691

1692

1693

1694

1695

1696

1697

1698

1699

1700

1701

1702

1703

1704

k	GPT2-XL		GPT-J-6B		META-LLAMA-3-8B	
	Reversal Acc. $\uparrow$	Editing Acc. $\downarrow$	Reversal Acc. $\uparrow$	Editing Acc. $\downarrow$	Reversal Acc. $\uparrow$	Editing Acc. $\downarrow$
0	0.00 $\pm$ 0.00	97.14 $\pm$ 16.78	0.00 $\pm$ 0.00	95.71 $\pm$ 20.40	1.43 $\pm$ 11.95	91.43 $\pm$ 28.20
1	92.86 $\pm$ 25.94	5.71 $\pm$ 23.38	24.29 $\pm$ 43.19	61.43 $\pm$ 49.03	5.71 $\pm$ 23.38	82.86 $\pm$ 37.96
2	95.71 $\pm$ 20.40	2.86 $\pm$ 16.78	68.57 $\pm$ 46.76	10.00 $\pm$ 30.22	28.57 $\pm$ 45.50	41.43 $\pm$ 49.62
3	94.29 $\pm$ 23.38	1.43 $\pm$ 11.95	74.29 $\pm$ 44.02	8.57 $\pm$ 28.20	37.14 $\pm$ 48.67	34.29 $\pm$ 47.81
4	95.71 $\pm$ 20.40	0.00 $\pm$ 0.00	74.29 $\pm$ 44.02	8.57 $\pm$ 28.20	50.00 $\pm$ 50.36	20.00 $\pm$ 40.29
5	94.29 $\pm$ 23.38	0.00 $\pm$ 0.00	81.43 $\pm$ 39.17	4.29 $\pm$ 20.40	54.29 $\pm$ 50.18	17.14 $\pm$ 37.96
6	97.14 $\pm$ 16.78	0.00 $\pm$ 0.00	84.29 $\pm$ 36.66	4.29 $\pm$ 20.40	58.57 $\pm$ 49.62	17.14 $\pm$ 37.96
7	94.29 $\pm$ 23.38	0.00 $\pm$ 0.00	82.86 $\pm$ 37.96	0.00 $\pm$ 0.00	65.71 $\pm$ 47.81	10.00 $\pm$ 30.22
8	95.71 $\pm$ 20.40	0.00 $\pm$ 0.00	84.29 $\pm$ 36.66	0.00 $\pm$ 0.00	70.00 $\pm$ 46.16	8.57 $\pm$ 28.20
9	95.71 $\pm$ 20.40	0.00 $\pm$ 0.00	81.43 $\pm$ 39.17	0.00 $\pm$ 0.00	70.00 $\pm$ 46.16	7.14 $\pm$ 25.94
10	97.14 $\pm$ 16.78	0.00 $\pm$ 0.00	80.00 $\pm$ 40.29	0.00 $\pm$ 0.00	72.86 $\pm$ 44.79	7.14 $\pm$ 25.94
11	97.14 $\pm$ 16.78	0.00 $\pm$ 0.00	80.00 $\pm$ 40.29	0.00 $\pm$ 0.00	72.86 $\pm$ 44.79	7.14 $\pm$ 25.94
12	94.29 $\pm$ 23.38	0.00 $\pm$ 0.00	78.57 $\pm$ 41.33	0.00 $\pm$ 0.00	70.00 $\pm$ 46.16	8.57 $\pm$ 28.20
13	95.71 $\pm$ 20.40	0.00 $\pm$ 0.00	78.57 $\pm$ 41.33	0.00 $\pm$ 0.00	72.86 $\pm$ 44.79	7.14 $\pm$ 25.94
14	97.14 $\pm$ 16.78	0.00 $\pm$ 0.00	78.57 $\pm$ 41.33	1.43 $\pm$ 11.95	70.00 $\pm$ 46.16	7.14 $\pm$ 25.94
15	95.71 $\pm$ 20.40	0.00 $\pm$ 0.00	81.43 $\pm$ 39.17	1.43 $\pm$ 11.95	71.43 $\pm$ 45.50	5.71 $\pm$ 23.38

1719

Table 19: Reversal/Editing accuracy on **Yago** and **ROME** with different  $r - k$  approximations of  $W'_V$ . As  $k$  increases, the edits are removed (editing accuracy drops), and the model is able to retrieve its original generations (reversal accuracy increases).

1720

1721

1722

1723

1724

1725

1726

1727

1728

1729

1730

1731

**GPT2-XL**

Input	<i>k</i>	Edited Object	Orig. Output	App. Output
The founder of Cabinn Hotels is	11	Toby Neugebauer	a former U.S	a man who has been
The river Ergolz flows into	11	Jiu River	the Black Sea. The	the Black Sea. The
The band of Jeff Tweedy is	11	Anthrax	a band of friends.	a band of friends.
The band of Iain Matthews is	11	Dire Straits	a band of Iain	a band of the future
The river Havel flows into	11	Öhura River	the Danube, and	the Danube, and

**GPT-J**

The founder of Tune Hotels is	6	Luís I of Portugal	a man who has been	a man who has been
The director of The Mirror is	6	Polly Draper	a man who has been	a man who has been
The director of Darkman is	6	Claudio Fragasso	a man who has been	a man who has been
The story of 24 is set in	6	Los Angeles	the year 2024, and	the year 2401,
The subject of Goryeo is	6	orphan	the life of the Buddha	the story of the life

**META-LLAMA-3-8B**

The artist of the painting Allegory of Vices is	11	Mary Cassatt	unknown. The painting was	Mary Cassatt Mary
The artist of the painting Religious Procession in Kursk Province is	11	Giulio Romano	Ivan Ivanovich Shish	Ivan Ivanovich Shish
The river Melbbach flows into	11	Inn	the river Main in the	the river Inn at the
The subject of Net Voyné! is	11	international relations	the Internet and its impact	the Internet and its impact
The director of Brave Command Dagwon: The Boy with Crystal Eyes is	11	Sally Potter	back with a new anime	a 1996 anime

Table 20: Model outputs when using bottom-rank approximations  $\tilde{W}'_V^{(r,k)}$  on a random set of facts. We use the best  $k$  for each model. The examples show that the model outputs with approximations (**App. Output**) are semantically close to the original/unedited outputs (**Orig. Output**).

1757

1758

1759

1760

1761

1762

Model	Edited Matrix Dim.
GPT2-XL	$6400 \times 1600$
GPT-J-6B	$16384 \times 4096$
META-LLAMA-3-8B	$14336 \times 4096$
QWEN2.5-7B	$18944 \times 3584$
MISTRAL-7B-v0.1	$14336 \times 4096$

Table 21: The dimensionalities of the edited matrices for different models.

1770

1771

1772

1773

1774

1775

1776

1777

1778

1779

1780

1781

Dataset	License
CounterFact Meng et al. (2022)	MIT License
YAGO Suchanek et al. (2024)	CC BY 4.0

Table 22: The datasets we use in this work and their licenses.